

A hybrid FETI-DP method for non-smooth random partial differential equations

Martin Eigel, Robert Gruhlke

submitted: December 21, 2018

Weierstrass Institute
Mohrenstr. 39
10117 Berlin
Germany
E-Mail: martin.eigel@wias-berlin.de
robert.gruhlke@wias-berlin.de

No. 2565
Berlin 2018



2010 *Mathematics Subject Classification.* 35R60, 47B80, 60H35, 65C20, 65N12, 65N22, 65N55, 65J10.

Key words and phrases. Elliptic pde, partial differential equations with random coefficients, domain decomposition, FETI, non-smooth, uncertainty quantification, stochastic finite element method.

The authors gladly acknowledge the funding of RG in the DFG SPP 1886 “Polymorphic uncertainty modelling for the numerical design of structures”.

Edited by
Weierstraß-Institut für Angewandte Analysis und Stochastik (WIAS)
Leibniz-Institut im Forschungsverbund Berlin e. V.
Mohrenstraße 39
10117 Berlin
Germany

Fax: +49 30 20372-303
E-Mail: preprint@wias-berlin.de
World Wide Web: <http://www.wias-berlin.de/>

A hybrid FETI-DP method for non-smooth random partial differential equations

Martin Eigel, Robert Gruhlke

Abstract

A domain decomposition approach exploiting the localization of random parameters in high-dimensional random PDEs is presented. For high efficiency, surrogate models in multi-element representations are computed locally when possible. This makes use of a stochastic Galerkin FETI-DP formulation of the underlying problem with localized representations of involved input random fields. The local parameter space associated to a subdomain is explored by a subdivision into regions where the parametric surrogate accuracy can be trusted and where instead Monte Carlo sampling has to be employed. A heuristic adaptive algorithm carries out a problem-dependent hp refinement in a stochastic multi-element sense, enlarging the trusted surrogate region in local parametric space as far as possible. This results in an efficient global parameter to solution sampling scheme making use of local parametric smoothness exploration in the involved surrogate construction. Adequately structured problems for this scheme occur naturally when uncertainties are defined on sub-domains, e.g. in a multi-physics setting, or when the Karhunen-Loève expansion of a random field can be localized.

The efficiency of this hybrid technique is demonstrated with numerical benchmark problems illustrating the identification of trusted (possibly higher order) surrogate regions and non-trusted sampling regions.

1 Introduction

In Uncertainty Quantification (UQ), numerical methods typically are either based on pointwise sampling, which is applicable to quite general problems but rather inefficient, or they rely on (an often analytic) smoothness of the parameter to solution map with the parameters determining the randomness. However, in many science and engineering applications deviating from the common Darcy benchmark setting with smooth Karhunen-Loève random fields, higher smoothness cannot be assumed globally in the parameter domain. This severely limits the use of techniques relying on sparsity or low-rank approximability.

As a prototypical application example, which is for instance of great relevance in material science, we have in mind a composite material with random non-periodic inclusions. This setting exhibits discontinuities in the parameter dependence, rendering it basically intractable to functional approximations with global basis functions in parameter space as commonly used in Stochastic Galerkin FEM, Stochastic Collocation and other non-intrusive projection approaches.

While Monte Carlo sampling and its modern variants (e.g. Quasi and Multilevel Monte Carlo) provide a widely applicable and robust approach, smoothness can only be used to a limited extent, resulting in slow convergence in the number of samples. Nevertheless, for problems with low parameter regularity, a sampling approach might seem the only option to pursue.

A notion not frequently used for this kind of problems is a localization of randomness as e.g. by means of a domain decomposition method, which is the basis for this work. In fact, the guiding principle is to make the high-dimensional problem more accessible by considering smaller physical domains, leading to a dependence on fewer relevant random variables locally. However, since the local representations cannot be assumed independent from each other, a weak coupling condition has to be introduced. To achieve this, we rely on the well-known theory of domain decomposition techniques and in particular the class of FETI and FETI-DP methods, see e.g. [31, 30, 29]. These methods have also been investigated for random problems e.g. in [44, 10, 24]. For more details and references we refer to Section 4. To develop these approaches further, we introduce the concept of *trust* and *no-trust regions* for a prescribed error tolerance [24] locally in which the highly efficient surrogate can be evaluated (“trusted”) or where one has to fall back to standard pointwise sampling. Local surrogates can be generated in parallel and depend only on local random coordinates. In order to get the largest gain from the construction, trust regions are required to cover as large an area of each subdomain as possible. For this, we introduce a local generalized multi-element discretization, for which a hp adaptive refinement procedure based on error indicators is presented.

The proposed hybrid stochastic FETI-DP allows for fast global sampling on the basis of local smoothness exploitation by appropriate surrogates.

The paper is structured as follows: The next section introduces the considered linear random model problem and provides an overview of the perturbation and convergence theory in particular for the case motivating this work, namely non-smooth coefficients. Section 3 examines the construction of surrogate models, which are used locally in the method. Special attention is paid to generalized multi-element polynomial chaos expansions and a partition of unity interpolation. The employed parametric domain decomposition method is derived in Section 4, which leads to a parametric FETI-DP method central to our approach. Eventually, Section 5 demonstrates the accuracy and adaptive refinement behaviour of the hybrid sampling approach based on some benchmark problems.

2 Model problem and a-priori estimates

In this section we introduce the random linear elliptic model problem used henceforth for the derivation of the proposed domain decomposition method. Of particular interest is the effect of approximation errors of the coefficient. We examine conditions for stability results of the approximate solution especially in the case of non-smooth coefficients. An application we have in mind is the numerical treatment of stochastic composite materials. This type of problem is much more involved than the frequently considered case of random PDEs with smooth data as e.g. presented in [2, 3, 12, 15, 16], where the dependence on the countable (possibly infinite) parameter vector is analytic. Such a very smooth dependence allows for the derivation of best n -term approximations with optimal (exponential) convergence rates and, while still very costly computationally, the implementation of numerical methods, respectively.

For the reader mainly interested in the proposed hybrid sampling approach, we suggest to skim through this section to understand the examined model problem and the structure of non-smooth problems in the examples provided at the end.

2.1 Concrete Random PDE Model

As model problem we consider a random linear partial differential equation. Given a probability space $(\Omega, \mathcal{U}, \mathbb{P})$, a LIPSCHITZ domain $D \subset \mathbb{R}^d$ with $d = 2, 3$, and Dirichlet and Neumann boundary segments $\Gamma_0, \Gamma_1 \subset \partial D$ with $\partial D = \Gamma_0 \cup \Gamma_1$, $\Gamma_1 \cap \Gamma_0 = \emptyset$ and $|\Gamma_0| > 0$. Then, the stationary diffusion model equation reads pointwise for $\omega \in \Omega$ a.e.

$$\begin{cases} -\operatorname{div} A(x, \omega) \nabla u(x, \omega) &= f(x, \omega) & \text{in } D, \\ \mathbf{n}^T A(x, \omega) \nabla u(x, \omega) &= g(x, \omega) & \text{on } \Gamma_1, \\ u(x, \omega) &= 0 & \text{on } \Gamma_0. \end{cases} \quad (1)$$

In the following we state natural pathwise and global assumptions in the setting of elliptic (pathwise) second order PDEs. In the context of integrability we use small letters for physical integrability and big letters for stochastic integrability.

(PA1) For a.e. $x \in D$, $\omega \in \Omega$, the $d \times d$ matrix $A(x, \omega)$ is symmetric and positive definite. Denote by $\lambda_{\min/\max}(A(x, \omega))$ the smallest and largest eigenvalue of $A(x, \omega)$ and define

$$\begin{aligned} \lambda_{\min}(A(\cdot, \omega)) &:= \operatorname{ess\,inf}_{x \in D} \lambda_{\min}(A(x, \omega)), \\ \lambda_{\max}(A(\cdot, \omega)) &:= \operatorname{ess\,sup}_{x \in D} \lambda_{\max}(A(x, \omega)). \end{aligned}$$

Then there exists $\underline{c}, \bar{c}: \Omega \rightarrow \mathbb{R}$ such that there hold pathwise uniform bounds a.e. in ω ,

$$0 < \underline{c}(\omega) \leq \lambda_{\min}(A(\cdot, \omega)) \leq \lambda_{\max}(A(\cdot, \omega)) \leq \bar{c}(\omega) < \infty. \quad (2)$$

(PA2) The random variable $\underline{c}(\omega)^{-1}$ is an element of $L^R(\Omega)$ for some $R \in [1, \infty]$.

(A1) There exists $c > 0$ such that $0 < c < \underline{c}(\omega)/\bar{c}(\omega) \leq 1$, a.e. in Ω .

(A2) Uniform bounds: $0 < \underline{C}, \bar{C} < \infty$ such that $\operatorname{ess\,inf} \underline{c}(\omega) \geq \underline{C}$ and $\operatorname{ess\,sup} \bar{c}(\omega) \leq \bar{C}$.

(A3) As a standard assumption we have $g \in L^P(\Omega; H_{00}^{-1/2}(\Gamma_1))$ (cf. [43]) and $f \in L^P(\Omega; (H_{\Gamma_0}^1)^*)$ for some $P \in [1, \infty]$.

Remark 2.1. Note that the uniform bound assumption (A2) is not necessary for pathwise existence and uniqueness of a weak solution. However, it turns out to be useful for used interpolation arguments and the p -condition with $p \neq p(\omega)$.

We define the pathwise bilinear form \mathcal{A} for a coefficient B satisfying pathwise assumptions (PA1)–(PA2),

$$\mathcal{A}[B, \omega](w, v) := \int_D B(x, \omega) \nabla w(x) \cdot \nabla v(x) \, dx, \quad \forall w, v \in H_{\Gamma_0}^1(D),$$

and the pathwise linear form

$$\ell[\omega](v) := \int_D f(x, \omega) v(x) \, dx + \int_{\Gamma_1} g(\omega, x) v(x) \, ds, \quad \forall v \in H_{\Gamma_0}^1(D).$$

Then the pathwise weak formulation given B reads

$$\text{Seek } u(\omega) \in H_{\Gamma_0}^1(D) \text{ s.t. } a[B, \omega](u(\omega), v) = \ell[\omega](v), \quad \forall v \in H_{\Gamma_0}^1(D). \quad (\mathbf{P}_B)$$

Lemma 2.2. [6] Under assumptions (PA1)–(PA2) and (A3) there exists a unique pathwise weak solution $u(\omega) \in H_{\Gamma_0}^1(D)$ of (\mathbf{P}_B) with $B = A$ for \mathbb{P} -almost all $\omega \in \Omega$ with $u \in L^S(\Omega; H_{\Gamma_0}^1)$ with $1/S = 1/P + 1/R$.

2.2 Error estimate for coefficient approximate solutions

Let \hat{A} be some perturbation of A in (1), e.g. introduced by some quadrature scheme in the discretization process. Let u and \hat{u} be (pointwise) weak solutions with respect to A and \hat{A} . Then we are interested in the distance of u to \hat{u} in the abstract sense of

$$u \rightarrow \hat{u} \quad \text{if} \quad A \rightarrow \hat{A} \quad (3)$$

where the type of convergence has to be determined.

2.2.1 Pathwise error estimates

Let $u(\omega)$ be the solution of (\mathbf{P}_B) with $B = A$ and let $\hat{u}(\omega)$ be the solution of (\mathbf{P}_B) with $B = \hat{A}$. Denote by $\hat{c}: \Omega \rightarrow \mathbb{R}$ the lower bound random variable with respect to \hat{A} satisfying assumptions (PA1)–(PA2). For simplicity, we shall assume that the right-hand side linear form can be evaluated exactly. A standard observation is that

$$a[A, \omega](u(\omega), v(\omega)) = a[\hat{A}, \omega](\hat{u}(\omega), v(\omega)). \quad (4)$$

Inserting $0 = \hat{A}(x, \omega) \nabla u(x) - \hat{A}(x, \omega) \nabla u(x, \omega)$ one obtains

$$a[\hat{A}, \omega](u(\omega) - \hat{u}(\omega), v(\omega)) = a[A - \hat{A}, \omega](u(\omega), v(\omega)). \quad (5)$$

Now taking $v = u - \hat{u}$ and due to the assumptions on A the left-hand side can be estimated from below by

$$\hat{c}(\omega) \|u - \hat{u}\|_{H_{T_0}^1}^2 \leq \left| a[\hat{A}, \omega](u(\omega) - \hat{u}(\omega), u(\omega) - \hat{u}(\omega)) \right|. \quad (6)$$

Let us assume that $\nabla u(\omega)$ is in $L^p(D)$ for some $p \geq 2$. Then for q such that $1/p + 1/q = 1$, $q = 2p/(2-p) \in [2, \infty]$, we obtain pathwise

$$\left| a[A - \hat{A}, \omega](u(\omega), v(\omega)) \right| \leq \|A(\cdot, \omega) - \hat{A}(\cdot, \omega)\|_{L^q(D)} \|\nabla u(\omega)\|_{L^p(D)} \|\nabla v(\omega)\|_{L^2(D)}. \quad (7)$$

Combining (6) and (7) yields

$$\|u(\omega) - \hat{u}(\omega)\|_{H_{T_0}^1(D)} \leq \hat{c}(\omega)^{-1} \|A(\cdot, \omega) - \hat{A}(\cdot, \omega)\|_{L^q(D)} \|\nabla u(\omega)\|_{L^p(D)}. \quad (8)$$

Based on this derivation we can refine the above statement to a decomposition of the physical domain D with relaxed integrability requirements per subdomain of ∇u .

Lemma 2.3. (local perturbation) Let $\overline{D} = \overline{\cup_{s=1}^S D^s}$ with piecewise disjoint D_s . For $s = 1, \dots, S$, assume that $[\nabla u]_{|D^s}(\omega) \in L^{p_s}(D_s)$ for $p_s \geq 2$ for a.e. $\omega \in \Omega$ and let $q_s = 2p_s/(p_s - 2)$. Then,

$$\|u(\omega) - \hat{u}(\omega)\|_{H_{T_0}^1(D)} \leq \hat{c}(\omega)^{-1} \left[\sum_{s=1}^S \|\nabla u(\omega)\|_{L^{p_s}(D_s)} \|A(\omega) - \hat{A}(\omega)\|_{L^{q_s}(D_s)} \right]. \quad (9)$$

For $p_s \equiv 2$, the perturbation result recovers the standard L^∞ coefficient estimates. We are left with the question of integrability of ∇u . Here, we state a pathwise p^* -condition motivated by [7] in our random framework:

Definition 2.4. (p^* -condition)

For an integrability constant $p^* = p^*(A, d, D) > 2$ independent of ω , i.e. $p^* \neq p^*(\omega)$ and for $2 \leq p < p^*$ there is a conormal derivative trace space $X^p(\Gamma_1) := X(p, \Gamma_1, \Gamma_0)$. Furthermore for $g(\omega) \in X^p$, $f(\omega) \in W_{\Gamma_0}^{1,p}(D)^*$ and $u(\omega) \in W_{\Gamma_0}^{1,p}(D)$ and a random variable $C_p(\omega) = C_p(d, A, D)(\omega)$ it holds

$$\|\nabla u(\omega)\|_{L^p(D)} \leq C_p(\omega) \left(\|f(\omega)\|_{W_{\Gamma_0}^{1,p}(D)^*} + \|g(\omega)\|_{X^p(\Gamma_1)} \right) \quad (10)$$

Here $X^p(\Gamma_1) \subset W^{-\frac{1}{p},p}(\Gamma_1)$ is a closed subspace with equality if $\Gamma_0 = \emptyset$ respecting DIRICHLET data in the spirit of LIONS-MAGENES space $H_{00}^{-1/2}(\Gamma_1)$ [45] obtained by interpolation [47] as the dual of the space $[W_0^{1,p'}, L^{p'}]_{1/p,p}$ with $1/p + 1/p' = 1$ defined on the NEUMANN boundary.

We emphasize the most common setting with $p = 2$ and $q = \infty$. In this HILBERTIAN case, $C_2(\omega) = \underline{c}(\omega)^{-1}C(D)$ with \underline{c} from Assumption (PA1) and constant $C(D)$ only depends on D , i.e. it is determined by POINCARÉ and trace inequality constants.

For $p > 2$ the verification of this condition is somewhat more involved but fortunately still holds true. In the case of a purely homogeneous Dirichlet boundary for the plain Laplacian with $A = I$, for any Lipschitz domain it follows by [28] that there exist $\bar{p}^* = \bar{p}^*(d, D) > 3$ ($\bar{p}^* > 4$ for $d = 2$) and a constant $K = K(\bar{p}^*, D)$ such that for all $2 \leq p \leq \bar{p}^*$

$$\|\nabla u(\omega)\|_{L^p(D)} \leq K \|f(\omega)\|_{W_{\Gamma_0}^{1,p}(D)^*}. \quad (11)$$

The result extends to $A(\omega) \neq I$ by a perturbation argument (see [35, 7]) and can in particular be translated to our pathwise framework. In this context there exists a function $p^*: (0, 1) \rightarrow (2, P)$ defined by

$$p^*(t) := \operatorname{argmax}\{K^{-\eta(p)} > 1 - t : 2 < p < \bar{p}^*\} \quad (12)$$

with $\eta(p) := (1 - 2/p)/(1 - 2/\bar{p}^*) \in (0, 1)$ monotonously increasing. With this construction, there are random variables

$$\bar{p}^*(\omega) := p^*(\underline{c}(\omega)/\bar{c}(\omega)), \quad C_p(\omega) := \frac{1}{\bar{c}(\omega)} \frac{K^{\eta(p)}}{1 - K^{\eta(p)}(1 - \underline{c}(\omega)/\bar{c}(\omega))}, \quad (13)$$

depending on the random variable bounds \underline{c}, \bar{c} of A from (PA1). An important observation is that $p^*(t)$ is monotonously decreasing in t . With this construction in mind, let $u(\omega)$ be the pathwise solution of (\mathbf{P}_B) with $B = A$ satisfying Assumption (PA1). Then for \mathbb{P} -a.a. ω in Ω and $2 \leq p < p^*(\underline{c}(\omega)/\bar{c}(\omega))$ pathwise it holds

$$\|\nabla u(\omega)\|_{L^p(D)} \leq C_p(\omega) \|f(\omega)\|_{W_{\Gamma_0}^{1,p}(D)^*}. \quad (14)$$

Hence, in order to satisfy the p^* -condition in Definition 2.4 the quotient $\underline{c}(\omega)/\bar{c}(\omega)$ needs to be bounded away from zero to have $\operatorname{ess\,inf} \bar{p}^*(\omega) > 0$, which motivates our Assumption (A1). This result is summarized in the following theorem.

Theorem 2.5. Assume $|\Gamma_1| = \emptyset$. Let $f(\omega) \in W^{-1,p}(D)$ and $u(\omega) \in W_0^{1,p}(D)$ the corresponding solution of (\mathbf{P}_B) with $B = A$ satisfying (PA1), (PA2) and (A1) with $2 \leq p < p^* := p^*(c)$ for $c > 0$ from (A1). Then the p^* -condition holds true.

Note that the uniform boundedness Assumption (A2) implies (A1). The case of mixed boundary conditions and L^p estimates of solution gradients can be derived from results of [23]. $W^{1,p}(D)$ estimates for ROBIN boundary conditions can be obtained from [1] with boundary right hand side in $W^{-\frac{1}{p},p}(\partial D)$ requirements.

We end the pathwise discussion of this section with an examination of the (p, q) relation. There are two important cases:

- 1 $q = \infty$, thus $p = 2$: As in the standard uniform bound. In order to have pathwise $\hat{u}(\omega) \rightarrow u(\omega) \in H_{T_0}^1(D)$, we need that $\hat{A}(\omega) \rightarrow A(\omega)$ in $L^\infty(D)^{d,d}$. From a practical point of view, i.e. when \hat{A} is due to the chosen discretization, we require more regularity of $A(\cdot, \omega)$ with respect to the physical coordinate x in order to bound the L^∞ error.
 - $A(\cdot, \omega) \in C^{k,\alpha}(D)$ yields an error of $\mathcal{O}(h^k)$ with an appropriate quadrature scheme.
 - If $A(\cdot, \omega)$ is piecewise $\mathcal{C}^{k,\alpha}$ and resolved in a discretization (e.g. adapted meshing) process then the same is valid by the estimate above.
- 2 $q < \infty$, thus $p > 2$: This case is important if $A(\cdot, \omega)$ *lacks spatial regularity or cannot be resolved in a discretisation step* by some \hat{A} such that the error in the L^∞ norm stays $\mathcal{O}(1)$. In this case the $q = \infty, p = 2$ estimate might become meaningless. However, the p^* -condition still ensures convergence of the perturbed solution based on weaker approximation requirements on the coefficient. At this point one may ask for the approximation in the weakest norm possible, that is $q = 2$ such that

$$\|A(\omega) - \hat{A}(\omega)\|_{L^2(D)^{d,d}} \rightarrow 0 \quad \Rightarrow \quad \|u(\omega) - \hat{u}(\omega)\|_{H_{T_0}^1(D)} \rightarrow 0. \quad (15)$$

We note that this indeed is possible by an interpolation argument, assuming that A and \hat{A} satisfy the uniform boundedness (PA1) and (A2). Then,

$$\|A(\omega) - \hat{A}(\omega)\|_{L^q(D)^{d,d}} \leq C(q) \|A(\omega) - \hat{A}(\omega)\|_{L^2(D)^{d,d}}^{1/q}, \quad (16)$$

with a constant $C(q) = C(q, \|A - \hat{A}\|_{L^\infty})$. Since $\hat{A}(\omega)$ and $A(\omega)$ are assumed to be in $L^\infty(D)^{d,d}$, we obtain by interpolation that

$$\|A(\omega) - \hat{A}(\omega)\|_{L^q(D)^{d,d}} \leq C(q) \|A(\omega) - \hat{A}(\omega)\|_{L^2(D)^{d,d}}^{1/q}. \quad (17)$$

As a consequence in order to have control of a pathwise good approximation $\hat{u}(\omega)$ of $u(\omega)$, it is sufficient to control the L^2 approximation $\hat{A}(\cdot, \omega)$ of $A(\cdot, \omega)$. However, we note that by the employed interpolation this estimate introduces a reduced convergence order by a factor $1/q$. Hence, ideally one can strive for an L^q approximation to avoid a degeneration of the convergence order.

2.2.2 Global error estimates

We now analyse the effect of distance measurement of \hat{A} to A to the whole solution \hat{u} to u . More specifically, we are interested in an estimate of the form

$$\|u - \hat{u}\|_1 \leq h(\|A - \hat{A}\|_2) \quad (18)$$

with continuous $h : \mathbb{R}^+ \rightarrow \mathbb{R}^+$ with $h(0) = 0$ and suitable norms $\|\cdot\|_1$ and $\|\cdot\|_2$ such that $u \xrightarrow{\|\cdot\|_1} \hat{u}$ if $\hat{A} \xrightarrow{\|\cdot\|_2} A$. We state the main result of this subsection.

Theorem 2.6. (A-priori $L^q(D)$ -perturbation estimate)

Let $P, Q, R_1, R_2 \in [1, \infty]$, such that $S := (1/P + 1/Q + 1/R_1 + 1/R_2)^{-1} \geq 1$ and let the p^* -condition of Definition 2.4 hold. For $2 \leq p < p^*$ assume $C_p(\cdot) \in L^{R_2}(\Omega)$ and let $f \in L^P(\Omega; W_{\Gamma_0}^{1,p}(D)^*)$ and $g \in L^P(\Omega; X_{\Gamma_1}^p)$. Let $u(\omega)$ and $\hat{u}(\omega)$ be the unique solution from (\mathbf{P}_B) , with $B = A$ and $B = \hat{A}$, respectively, satisfying assumptions (PA1)–(PA2) with $R = R_1$. If $A, \hat{A} \in L^Q(\Omega; L^q(D))$ for $q = 2p/(2 - p)$ such that \hat{A} satisfies (PA1) with lower bound $\hat{c}(\cdot)^{-1} \in L^{R_1}(\Omega)$, then

$$\|u - \hat{u}\|_{L^S(\Omega; H_{\Gamma_0}^1(D))} \leq C \|A - \hat{A}\|_{L^Q(\Omega; L^q(D))}, \quad (19)$$

with $C = C(C_p, \hat{c}, f, g)$.

Proof. By (8) and the p^* -condition it holds pathwise that

$$\begin{aligned} \|u(\omega) - \hat{u}(\omega)\|_{H_{\Gamma_0}^1} &\leq \hat{c}(\omega)^{-1} \|A(\omega) - \hat{A}(\omega)\|_{L^q(D)} \|\nabla u(\omega)\|_{L^p(D)} \\ &\leq \hat{c}(\omega)^{-1} C_p(\omega) \|A(\omega) - \hat{A}(\omega)\|_{L^q(D)} \\ &\quad \times \left(\|f(\omega)\|_{W_{\Gamma_0}^{1,p}(D)^*} + \|g(\omega)\|_{X^p(\Gamma_1)} \right). \end{aligned}$$

The result then follows by multiple applications of the HÖLDER inequality. For example, choose α such that $Q = \alpha T$ and denote by α' its conjugate exponent. Then, skipping the pathwise dependence, this yields

$$\begin{aligned} \|u - \hat{u}\|_{L^T(\Omega; H_{\Gamma_0}^1(D))}^T &\leq \left\| \hat{c}^{-1} C_p \|A - \hat{A}\|_{L^q(D)} \right\|_{L^{T\alpha'}(\Omega)}^T \\ &\quad \times \left\| (\|f\|_{W_{\Gamma_0}^{1,p}(D)^*} + \|g\|_{X^p(\Gamma_1)}) \right\|_{L^Q(\Omega)}^T. \end{aligned}$$

Further iterative application of HÖLDER estimates yield the desired result. \square

The a-priori perturbation estimation gives a qualitative statement of some closeness of the approximated to the true solution if the approximation error of the involved coefficient A is controlled. We point out that the important case of coefficients that are numerically approximated in $L^Q(\Omega, L^\infty)$ is included. However, note that in this case the need of a p^* -condition can be relaxed.

Corollary 2.7. (A-priori $L^\infty(D)$ -perturbation estimate)

Let $P, Q, R_1, R_2 \in [1, \infty]$ such that $S := (1/P + 1/Q + 1/R_1 + 1/R_2)^{-1} \geq 1$ and assume $f \in L^P(\Omega; H_{\Gamma_0}^1(D)^*)$ and $g \in L^P(\Omega; H_{00}^{-1/2}(\Gamma_1))$. Let $u(\omega)$ and $\hat{u}(\omega)$ be the unique solutions of (\mathbf{P}_B) with $B = A$ and $B = \hat{A}$ satisfying assumptions (PA1) and (PA2) with $R = R_1$ and $R = R_2$, respectively. Then, for $A, \hat{A} \in L^Q(\Omega; L^\infty(D))$ it holds

$$\|u - \hat{u}\|_{L^S(\Omega; H_{\Gamma_0}^1(D))} \leq C \|A - \hat{A}\|_{L^Q(\Omega; L^\infty(D))}. \quad (20)$$

While the assumptions in Corollary 2.7 are rather mild, the important case of random fields A representing *composite random materials with random inclusions* (to be examined in the following example) might nevertheless be excluded. If this type of materials is modeled pathwise by piecewise HÖLDER continuous or even smoother data then it fits in the setting of Theorem 2.6. We shall illustrate this line of thought with a small example.

Example 2.8. (Composite material)

Consider $D = [-1, 1]^d$ for $d = 2, 3$ and let $r \sim \mathcal{U}[0, R]$ and $R < \bar{R} < 1$ such that

$$\alpha(x, \omega) = \alpha(x, r(\omega)) = \kappa_1 \chi_{B_{r(\omega)}(\mathbf{0})}(x) + \kappa_2 (1 - \chi_{B_{r(\omega)}(\mathbf{0})}(x))$$

with the EUCLIDIAN centered ball of radius $r(\omega)$ denoted by $B_{r(\omega)}(\mathbf{0})$ and an indicator function χ , see Figure 1. In mesh based discretization schemes with standard piecewise polynomial root based quadrature, the spherical random interfaces and thus the jump of the coefficient $A(x, \omega) := \alpha(x, \omega)I$ cannot be approximated pathwise in $L^\infty(D)$. In particular, for any such finite quadrature scheme, by the GIBBS phenomenon this error is $\mathcal{O}(1)$ w.r.t. the L^∞ norm.

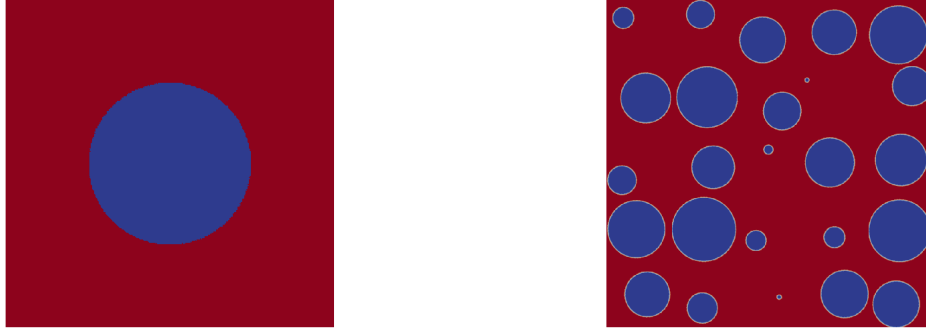


Figure 1: **Left:** Realization of composite material α ; **Right:** Realizations of varying composite with multiple separated inclusions.

Example 2.9. (Composite material approximation)

Given the tensor parameter domain $\Xi := [-1, 1]^{d+1}$ and a physical (reference) domain $\hat{D} = [0, 1]^d$, consider the mapping $\varphi : \Xi \rightarrow \mathcal{K}_\delta$ for some $0 < \delta \ll 1$ with

$$\mathbf{y} := (y_0, y_1, \dots, y_d) \mapsto \varphi(\mathbf{y}) = (r, \mathbf{p}) = (r, p_1, \dots, p_d)$$

and $\mathcal{K}_\delta = \{(r, \mathbf{p}) \in [0, R] \times D \mid r < \text{dist}(\mathbf{p}, \partial D) - \delta\}$ for $0 < R < \bar{R} < 1$. Then, define

$$D \times \Xi \ni (x, \mathbf{y}) \mapsto \alpha(x, \varphi(\mathbf{y})) = \kappa_1 \chi_{B_{r(\mathbf{p})}}(x) + \kappa_2 (1 - \chi_{B_{r(\mathbf{p})}}(x)) \quad (21)$$

modeling a circular inclusion with varying position and radius where the inclusion has a positive distance δ from the boundary ∂D . In a numeric simulation we may approximate this setting e.g. by the following approaches

- $\hat{\alpha}_{MC}$ is a pathwise projection of $\alpha(\cdot, \mathbf{y})$ to the piecewise constants on an underlying mesh,
- $\hat{\alpha}$ might be a cluster approximation, that is a piecewise constant approximation with respect to the parameter \mathbf{y} ,
- $\hat{\alpha}$ is implicitly approximated when surrogates in domain decomposition methods (like parameter dependent local Schur complements) are approximated continuously by piecewise affine functions.

These type approximations may not converge in $L^Q(\Xi; L^\infty(D))$. With the above construction of α and φ on a reference domain \hat{D} we can build a composite material with multiple varying inclusions defined on non-overlapping subdomains as illustrated in Figure 1 right.

Remark 2.10. The strong convergence assumption in $L^Q(\Omega; L^q(D))$ and the requirements of the p^* condition can be relaxed in the fully discretized setting. In fact, it only has to hold

$$U_\ell \subset U := L^2(\Omega; H_{\Gamma_0}^1(D)) \hookrightarrow H := L^2(\Omega, L^2(D)), \quad (22)$$

with $|U_\ell| < \infty$ on level $\ell \geq 0$. This holds true for example if a polynomial chaos expansion and a conforming FE discretization are employed and ℓ denotes an (adaptive or uniform) refinement level. Let

$$b[B](u, v) := \int_{\Omega} \int_D B(x, \omega) \nabla u(x, \omega) \cdot \nabla v(x, \omega) dx d\mathbb{P}. \quad (23)$$

In the discrete case, by STRANG's Lemma, one needs an estimate of

$$|b[A](w_\ell, v_\ell) - b[\hat{A}](w_\ell, v_\ell)| = |\langle A - \hat{A}, \nabla w_\ell \cdot \nabla v_\ell \rangle_H|. \quad (24)$$

Hence, for a fixed discretization level ℓ , we have $\nabla w_\ell \cdot \nabla v_\ell \in H$ and as a consequence it is sufficient to have that \hat{A} converges weakly to A in the H topology to control the error in (24). In particular, it suffices that $\hat{A} \rightarrow A$ strongly in H instead of stronger convergence in $L^2(\Omega; L^\infty(D))$ or $L^Q(\Omega; L^q(D))$, when starting from the discrete setting.

3 Surrogate response

The construction of surrogate models for problems with high-dimensional input (parameters) becomes essential when extensive sampling is computationally expensive in comparison to the construction of adequate functional approximations. These may even be viable for non-smooth data since it can still be possible to exploit local smoothness, which then would result in sufficiently accurate surrogates.

In the literature there is a vast amount of surrogate types, including generalized polynomial chaos expansions (gPCE), e.g. [49, 18], its multi-element extension, e.g. [48], low-rank [25, 21] or sparse grid techniques, e.g. [37, 22] or neural networks and references therein.

A central motivation for the proposed approach is the treatment of parametric composite materials. With this in mind, our aim is to build (local) surrogates for (local) maps within a domain decomposition framework presented in Section 4. For this, we focus on two surrogate types based on a parameter space decomposition, namely the *multi-element generalized polynomial chaos* expansion and a *partition of unity interpolation*. In the case of low-rank structures, also hierarchical tensor representations might become useful.

3.1 Surrogates for matrix valued functions

In preparation for the framework of localized descriptions of randomness in a domain decomposition setup we discuss different surrogate models for random matrices of the form

$$\xi^r(\omega) \mapsto M^s(\xi^r(\omega)), \quad (25)$$

with some matrix valued image $M(\xi^r(\omega)) \in \mathbb{R}^{n,m}$, $n, m \in \mathbb{N}$, for some indices $r, s \in \mathbb{N}$. In our application n and m depend on the number of interface degrees of freedom or subsets of these. The choice of surrogate for the map (25) should be made dependend on the regularity of the involved map. In particular, we have the following surrogates in mind that are based on L^2 best approximations or interpolations.

- 1 *hPCE surrogates*: An orthonormal discrete subspace of $L^2(\Gamma_r, \mathcal{B}(\Gamma_r), \mu_r)$ based on piecewise orthonormal polynomials with respect to μ_r is chosen. Then, the coefficients in the *hPCE* series are computed via projection, e.g. via a stochastic Galerkin method or (sparse) quadrature schemes. In this approach one might consider several separate subsurrogates for each column of $M(\cdot)_i$, $1 \leq i \leq m$.
- 2 *Hierarchical tensor surrogates*: A possibly low number of samples of M^s and a given underlying discrete tensor basis is provided. Then, a tensor reconstruction as in the (non-intrusive) *Variational Monte Carlo method* [17] yields a L^2 -compressed low-rank representation.
- 3 *PoU interpolation surrogates*: Based on an adaptive mesh of Γ_k , a discrete partition of unity basis with respect to the mesh is used. This can e.g. be obtained by a LAGRANGE basis with respect to mesh nodes. Then, each basis coefficient is computed by a single sample. More details are provided in Section 3.3.
- 4 *Sparse grid interpolation surrogates* are build by evaluating a realization of M^s on each sparse grid point.

Remark 3.1. In the case of low regularity of the map (25) and no knowledge of a basis for an approximation scheme with (quasi)-optimal convergence in the sense of ℓ^p -summability of coefficients for some $p \geq 1$ [4], we may be restricted to lower local parametric dimensions to obtain an affordable and accurate surrogate. While out of the scope of this paper, a progressive learning of an approximate basis as e.g. via a Neural Networks regression might become useful, given its training only involves a manageable number of samples. Regression based on neural networks or hierarchical tensor representations will be discussed elsewhere.

3.2 Generalized Multi-Element Polynomial Chaos Expansion

The following presentation is motivated by the approximation of non-smooth functions, where standard functional approaches may lack efficiency due to the GIBBS phenomenon.

We consider a probability measure μ on $\Gamma \subset \mathbb{R}^{M'}$ and the space $L^2(\Gamma, \mathcal{B}(\Gamma), \mu)$. For the envisaged application, Γ is the image and μ will be the push-forward of \mathbb{P} of an underlying parameter random vector \mathbf{I} , identified with some $\mathbf{y} = \mathbf{I}(\omega) \in \Gamma$. Let $\mathcal{I} = \mathbb{N}$ and assume that there exists a family of orthonormal polynomials $\Psi := \{\psi_\alpha\}_{\alpha \in \mathcal{I}}$ such that

$$\text{span}(\Psi) \stackrel{d}{\hookrightarrow} L^2(\Gamma, \mathcal{B}(\Gamma), \mu).$$

Note that if there exists $c > 0$ and a norm $\|\cdot\|$ on $\mathbb{R}^{M'}$ such that

$$\int_{\Gamma} e^{c\|\mathbf{y}\|} d\mu(\mathbf{y}) < \infty, \quad (26)$$

then such a family does indeed exist [11].

Example 3.2. The condition (26) holds for any bounded domain Γ or for $\Gamma = \mathbb{R}^{M'}$ and μ any GAUSSIAN measure, including the non-independent case [40].

In the special case that μ exhibits a product structure, i.e. the *independent case*, the index set \mathcal{I} can be reshaped into a multi-index tensor structure. To distinguish this special case from general measures, we use bold faced symbols and write $\Psi := \Psi(\mathcal{I}) := \{\psi_\alpha\}_{\alpha \in \mathcal{I}}$. The existence of a complete orthonormal polynomial basis may be answered by solving the one dimensional HAMBURGER moment problem [11].

Remark 3.3. There exist probability measures such that no dense polynomial subset exists. A classical example is the log-normal case. For $M' > 1$ and a non-separable probability measure μ or a non-tensorized domain Γ , such a family of polynomials might exist but is not necessarily unique [11]. For fixed α , the polynomial ψ_α inherits the product structure as

$$\Psi_\alpha = \prod_{i=1}^{M'} \Psi_{\alpha_i}.$$

We now consider a finite non-overlapping partition of $\Gamma = \bigcup_{k \in \mathcal{J}} \Gamma_k$ with $|\mathcal{J}| < \infty$, $\Gamma_k \in \mathcal{B}(\Gamma)$ and $0 < \mu(\Gamma_k) \leq 1$. This gives rise to the decomposition

$$Y := L^2(\Gamma, \mathcal{B}(\Gamma), \mu) = \bigoplus_{k \in \mathcal{J}} Y_k, \quad Y_k := \{v \in L^2(\Gamma, \mathcal{B}(\Gamma), \mu) : \text{supp}(v) \subset \Gamma_k\}.$$

Lemma 3.4. If Y can be spanned densely by orthonormal polynomials, then so can Y_k .

Proof. Fix $v \in Y_k$ and $\epsilon > 0$. Let χ_k denote the indicator function with respect to Γ_k , then $\varphi_{\alpha,k} := \chi_k \psi_\alpha$ for $\alpha \in \mathcal{I}$ is a polynomial in Y_k . Let Ψ_k be an orthonormalized version of $\Pi_k := \{\varphi_{\alpha,k}, \alpha \in \mathcal{I}\}$ with respect to the inner product in Y_k . Since Ψ is dense in Y , there exists $\mathcal{I}_\epsilon \subset \mathcal{I}$, $|\mathcal{I}_\epsilon| < \infty$ and a polynomial $\psi_\epsilon = \sum_{\alpha \in \mathcal{I}_\epsilon} c_{\epsilon,\alpha} \psi_\alpha \in \text{span } \Psi$ with

$$\|\mathbb{E}_0^k v - \psi_\epsilon\|_{L^2(\Gamma, \mathcal{B}(\Gamma), \mu)} < \epsilon.$$

Here, $\mathbb{E}_0^k: L^2(\Gamma_k) \rightarrow L^2(\Gamma)$ denotes the zero extension operator. Consequently $\|v - \chi_k \psi_\epsilon\|_{Y_k} < \epsilon$, where $\chi_k \psi_\epsilon \in \text{span } \Psi_k$. \square

Motivated by Lemma 3.4, we define an (weak) orthonormal polynomial set

$$\Psi_k := \{\psi_{\alpha,k}, \alpha \in \mathcal{I}, \psi_{\alpha,k} \text{ is polynomial}\}, \quad (\psi_{\alpha,k}, \psi_{\alpha',k})_{Y_k} = \delta_{\alpha,\alpha'}, \quad (27)$$

which spans a dense subset in Y_k . We note that in the independent case the decomposition of Γ has to respect the tensor structure to obtain a product structure of the polynomial chaos.

Lemma 3.5. If Y has a dense orthonormal polynomial subset then $\bigoplus_{k \in \mathcal{J}} \Psi_k$ spans a dense subset in Y with Ψ_k from (27).

Proof. The statement follows immediately since $v \in Y$ can be written as $v = \bigoplus_{k \in \mathcal{J}} v_k$ with $v_k = \chi_{\Gamma_k} v \in Y_k$ and an application of Lemma 3.4. \square

As the partition of Γ can be interpreted as a possibly non-regular meshing, we abbreviate the construction of polynomial chaos on several elements as *gHPCE*, motivated by hp-FEM in the standard Lebesgue spaces $L^2(D, d\lambda)$. For more details on the existence of dense generalized polynomial chaos we refer to [49, 18, 11].

We conclude this subsection with two instructive examples.

Example 3.6. (Construction of gHPCE) Consider the special case of $\Gamma \subset \mathbb{R}$ and denote by $\frac{d\mu}{dy} = \varrho$ the Radon-Nikodým derivative of μ with respect to the Lebesgue measure. Let $a_0 = \inf \Gamma < a_1 < \dots < a_{|\mathcal{J}|} := \sup \Gamma$. Based on the local inner product

$$\int_{a_k}^{a_{k+1}} u(y)v(y)\varrho(y)dy,$$

orthonormal families can be obtained by a GRAM-SCHMIDT procedure. In the case of a uniform distribution, the multi-element Legendre chaos can be obtained by simple rescaling and translation of standard Legendre chaos.

Example 3.7. If only samples of μ are known, an empirical gPC can be constructed with data driven approaches using moment reconstruction [39].

3.2.1 Hierarchical Tensor Trains and Tensor reconstruction

We assume that $L^2(\Gamma, \mathcal{B}, \mu)$ exhibits a product structure. Thus, the truncated gPC discretization basis functions can be written as a product of one dimensional piecewise polynomials. If the product structure is not given, a change of the coordinate system as e.g. realized via the Rosenblatt/Nataf transformation (approximated by transport maps [34]) yields a reparametrization into a coordinate system spanned by independent random variables. This is at the cost of introducing a non-linear transformation map, which has to be resolved. Then, any function $u \in L^2(\Gamma, \mathcal{B}, \mu)$ can be approximated by a tensor structured basis such that

$$u(\xi^r) \approx \sum_{\alpha, \mathbf{k}} C[\alpha, \mathbf{k}] \prod_{i,j} \Psi_{\alpha_i, k_j}(\xi_i^r). \quad (28)$$

Here, the multiindex $\alpha = (\alpha_1, \dots, \alpha_I)$ is related to the polynomial degree and $\mathbf{k} = (k_1, \dots, k_{|J|})$ is related to a tensorized decomposition of Γ , indexing a full tensor C . An approximation of such a tensor can be realized with hierarchical tensor formats, allowing for a compressed low-rank representation [21, 25, 5, 38], e.g. employing a tensor reconstruction or cross approximation algorithm.

3.3 Surrogates based on PoU-Interpolation

In the following, we consider the parametric matrix $\xi^r(\omega) \mapsto M^s(\xi^r(\omega))$. Let $\Gamma_r := \text{img } \xi^r$ and assume a nested set of discrete function spaces

$$U_{s,0}^r \subset U_{s,\ell}^r \subset \dots \subset U_{s,L}^r \quad (29)$$

of level $\ell = 0, 1, \dots, L$ defined by

$$U_{s,\ell}^r := \{\varphi_k^{s,\ell} : \Gamma_r \rightarrow \mathbb{R}, k = 1, \dots, N_\ell^i < \infty\} \quad (30)$$

such that its elements form a *partition of unity* (PoU) on Γ_r , i.e. $\sum_{k=1}^{N_\ell^i} \varphi_k^{s,\ell} \equiv 1$. To describe an important class of this spaces, we consider a family of cell partitions \mathcal{M}_ℓ^r of level $\ell = 1, \dots, L$ of Γ_r with tree structure: for each cell in $\mathcal{M}_{\ell+1}^r$ there is a unique father cell in \mathcal{M}_ℓ^r . Furthermore, assume that for each $k = 1, \dots, N_\ell$ the function $\varphi_k^{s,\ell}$ has support in one cell in $\mathcal{M}_{\ell+1}^r$ only, i.e.

$$\forall k = 1, \dots, N_\ell, \exists! T \in \mathcal{M}_\ell^r : \text{supp } \varphi_k^{s,\ell} \subset T. \quad (31)$$

Associate with each such function in $U_{s,\ell}^r$ a *global degree of freedom* and a unique associated element in Γ_r denoted by *global coordinate degree of freedom*.

We are now able to formulate an adaptive scheme to build up surrogates for the parametric matrix ensemble.

Algorithm 1: Hybrid surrogate based on a Partition of Unity

input : \circ sample routine \mathcal{S} for parametric matrix $M^s(\xi^r(\omega))$
 \circ surrogate quality parameter $\text{tol} > 0$
 \circ maximal level of refinement L

output: hybrid surrogate for $\xi^r(\omega) \mapsto M_i^s(\xi^r(\omega))$.

```

1 init  $M_0^r, U_{s,0}^r$ 
2 foreach  $\ell = 0, \dots, L$  do
3   markings := {}
4   trust region / non trust region :=  $\emptyset, \emptyset$ 
5   foreach global coordinate d.o.f of  $U_{s,\ell}^r$  do
6     evaluate  $\mathcal{S}$  and assign it to the corresponding global d.o.f.
7   foreach  $T \in M_\ell^r$  do
8     judge local quality of current surrogate on  $T$  with  $\text{tol}$ 
9     set  $T$  to be trusted / not trusted.
10    update trust region / non trust region with  $T$ 
11    if  $T$  is not trusted then
12      mark  $T$  in  $(M_\ell^r, U_{s,\ell}^r)$  for refinement, i.e. add to markings
13  if markings = {} then break
14  else
15     $M_{\ell+1}^r, U_{s,\ell+1}^r := \text{refine}(M_\ell^r, U_{s,\ell}^r, \text{markings})$ 
16 create hybrid surrogate that evaluates on space  $U_\ell^r$  for input lying within trust region and calls  $\mathcal{S}$  for input lying in non trust region.
```

The aim of the proposed Algorithm 1 is to balance the maximization the trust region while keeping the creation process as cheap as possible.

Remark 3.8. The hybrid structure, i.e. letting the surrogate coincide with a sample on the non trust region, allows to control the cost of creating the surrogate by L , which means overrefinement and thus too many sampler calls.

Remark 3.9. Although the above representation is presented for matrices, the technique also extends to matrices given only implicitly: If we are interested in building a surrogate for the inverse of $A(\xi(\omega))$, due to the partition of unity approach for each global coordinate degree of freedom we store a LU factorisation only. Then, the evaluation of the surrogate at a point p requires several forward-backward substitutions associated to all basis functions evaluating to non-zero at p . In the case of local supports this is a rather small number. Note that here each LU decomposition may have its own sparsity pattern determined by its pivotization and scaling. The extension of this approach to tensor formats is discussed elsewhere.

4 Parametric Domain decomposition

Based on an abstract partial differential equation model with possible high-dimensional random input decomposed w.r.t. to a physical partition, we present a domain decomposition method framework that yields to local problems with lower parametric dimensionality. Based on a semi-discretisation we introduce an accelerated sampling scheme in the spirit of [10] based on an adaptive construction of surrogates of local parameteric interface operators.

4.1 Abstract random domain decomposed model

Consider a partition of D into mutual disjoint, non-empty connected LIPSCHITZ subdomains $D^s \subset D$, $s = 1, \dots, N_{SD} < \infty$. We are interested in random fields given in parameterized form and possibly localized with respect to $(D^s)_s$. Such local representations of random fields may for instance occur in the following scenarios

- Localization to D^s via localized Karhunen-Loève expansions (e.g. [9]) in case of underlying GAUSSIAN random fields, see Example 4.2.
- Subdomain-wise uncertainties, e.g. random composite materials.

Instead of an abstract random field $a(x, \omega)$ we consider a parametrization by a given stochastic coordinate system, represented by some $\xi: \Omega \rightarrow \mathbb{R}^{M'}$, which means that $M' \in \mathbb{N} \cup \{\infty\}$. Let $\sigma(\xi) \subset \mathcal{U}$ be the sigma algebra generated by ξ and $(\Omega, \sigma(\xi), \mathbb{P})$ the considered space. Furthermore, assume a sub-enumeration of the M' -dimensional random vector ξ into $M \leq N_{SD}$ blocks of m_r -dimensional (sub) random vectors $\xi^r: \Omega \rightarrow \mathbb{R}^{m_r}$ with $1 \leq m_r \leq M'$ and components $\xi_i^r := (\xi^r)_i, i = 1, \dots, m_r, r = 1, \dots, M$. We are then interested in a physical model described by a linear partial differential equation with randomness modelled by ξ where at most one input random sub-vector ξ^r acts on a subdomain D_s as illustrated in Figure 2. If the latter is the case we call the tuple (r, s) an *active index*, which we collect in

$$\mathcal{I}_{\text{active}} := \{(r, s) \in \{1, \dots, M\} \times \{1, \dots, N_{SD} \mid (r, s) \text{ is active index}\}. \quad (32)$$

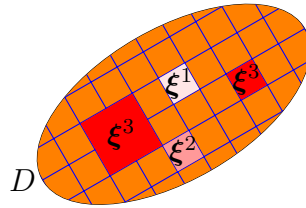


Figure 2: Parametric random input given by $M = 4$ sub random vectors $\xi^r, r = 1, \dots, 4$ distributed over different sub-structures.

The abstract equation reads

$$\mathcal{L}(\xi(\omega), x)u(\xi(\omega), x) = f(x), \text{ in } D, \quad (33)$$

$$\mathcal{B}(\xi(\omega), x)u(\xi(\omega), x) = g(x), \text{ on } \Gamma, \quad (34)$$

with $\mathcal{L}(\xi(\omega), x) = \mathcal{L}(\xi^r(\omega), x)$ for $x \in D^s$ for each $(r, s) \in \mathcal{I}_{\text{active}}$ from (32) and $\mathcal{L}(\xi(\omega), x) = \mathcal{L}(x)$ else. An analog structure holds for the boundary operator \mathcal{B} . Here, we assume existence and uniqueness of a solution $u \in L^2(\Omega, \sigma(\xi), \mathbb{P}) \otimes \mathcal{V}$ for some separable Hilbert space \mathcal{V} , e.g. $\mathcal{V} = H_{\Gamma_b}^1$ in the case of (1).

Note that the abstract model includes several important cases of random modeling:

- Direct modeling with independent random components, i.e. $(\xi^s)_s$ are mutually independent random vectors and \mathcal{L} is defined by material parameters that depend locally on ξ^r in a possible non-linear manner.

- The setting $\xi^r \equiv \xi$ corresponds to global random contributions, which includes the non-localized (standard) KLE case.
- The local coordinates ξ^r are obtained by a localized KLE. In the case that the underlying random field is GAUSSIAN, ξ and ξ^r consist of mutually independent GAUSSIAN random variable components, although now $(\xi^r)_r$ is not independent in general.
- The case of one localized uncertainty input $M = 1$ [8].

Remark 4.1. In order to balance the workload for parallel computations in the domain decomposition schemes introduced by varying sizes of subdomains described below, one might decompose a large subdomain, e.g. D^s , with operator dependence only on ξ^r , $(r, s) \in \mathcal{I}_{\text{active}}$ into $D^s = D^{s'} \cup D^{s''}$, thus updating $\mathcal{I}_{\text{active}}$ with (r, s') , (r, s'') instead of (r, s) . This might require involved system preconditioners since the material coefficient on the interface $D^{s'} \cap D^{s''}$ might behave non-trivially.

Example 4.2. (localized Karhunen-Loève expansion)

Given the mean and covariance kernel, a random field might be given as

$$a(x, \omega) = a(x, \boldsymbol{\eta}(\omega)) = a_0(x) + \sum_{i=1}^{\infty} \sqrt{\lambda_i} a_i(x) \eta_i(\omega), \quad x \in D,$$

with centered, uncorrelated random variables η_i and eigenpairs (λ_i, a_i) of the underlying covariance operator with respect to the full domain D . When considering the eigenvalue problem on subdomains D^s only, we obtain local representations in a new (larger) coordinate system $\xi = (\xi^s)_{s=1}^{N_{SD}}$ with sub-coordinates ξ^s , i.e.

$$a(x, \omega) = a(x, \xi^s(\omega)) = a_0(x) + \sum_{j=1}^{\infty} \sqrt{\lambda_j^s} a_j^s \xi_j^s(\omega), \quad x \in D^s.$$

Assume that the global KLE is truncated after M terms, yielding the desired accuracy. In the case that the local eigenvalues $(\lambda_j^s)_j$ have a (much) lower magnitude, the local KLE can be truncated after $m_s \ll M$ terms, i.e. a low dimensional local representation of the random field. Furthermore, there exists a matrix $A^s \in \mathbb{R}^{m_s, M}$ such that $(\eta_j^s)_{j=1}^{m_s} = A^s(\xi_i)_{i=1}^M$. In the case of GAUSSIAN random fields one gets the nice property that (η_j^s) are independent GAUSSIAN random variables as well, enabling local dense polynomial chaos approximations. Note that $(\xi^s)_s$ is not independent in general. This framework was introduced in [9].

Remark 4.3. Contrary to example 4.2, in the case that ξ_i are independent non-GAUSSIAN random variables, the distribution of $(\eta_j^s)_{j=1}^{m_s}$ can be arbitrarily complex since the involved linear map A^s introduces a non-linear mapping of distributions due to $m_s < M$. Hence, one cannot expect (η_j) to be independent and the existence of a dense polynomial chaos in $L^Q(\Omega, \sigma(\boldsymbol{\eta}), \mathbb{P})$ is not ensured in general, e.g. if $\text{img } \boldsymbol{\eta}_{m_s} \subset \mathbb{R}^{m_s}$ is unbounded. Note that the image might be of lower topological dimension, e.g. a submanifold only.

4.2 Parametric hybrid domain decomposition based on semi-discretisation

Domain decomposition generally refers to the splitting of a partial differential equation, or an approximation thereof, into coupled problems on smaller subdomains, forming a partition of the original domain, see [46]. We present the framework on a semi-discrete formulation with regard to some suitable

discrete subspace of \mathcal{V} . Then the structure of the decomposed random model (33)-(34) results in a random system of equations

$$\mathcal{A}(\xi(\omega))u(\xi(\omega)) = F(\xi(\omega)). \quad (35)$$

The domain decomposition approach for random partial differential equations is applied in the context of global and local Karhunen-Loève expansions in [44] and [10] with a combination of model reduction techniques [36] for the SCHUR complement or the FETI-DP method, respectively. We note that the technique based on global random coordinates is based on a Stochastic FE formulation without a sampling stage, which limits it to a small number of random coordinates due to the curse of dimensionality. To alleviate this issue, the aim is to rely on local random coordinates only, *e.g.* based on canonical tensor representations as in [26]. In what follows, we present both techniques, the SCHUR complement and the FETI-DP method based on local adaptively constructed surrogates that enable accelerated sampling. The general hybrid approach that we introduce is summarized in Algorithm 2.

Remark 4.4. If the local representation of $\mathcal{L}(\xi^r(\omega), x)$ is given by means of a gPCE with independent (ξ_k^r) then the involved local random operators may be represented in low-rank formats as in [14], allowing for higher dimensional local input. This approach transfers to compressed structures of all involved parametric suboperators. However, its discussion is out of the scope of this paper.

Algorithm 2: Abstract hybrid domain decomposition

input : ◦ number of total samples N
 ◦ local discrete physical spaces $V_{h,s}$
 ◦ surrogate cost bound C_\S and desired accuracy tol
output: Sample based approximation of some Q.o.I.(u)

```

1 foreach active pair  $(r, s)$  subdomain  $D^s$  in parallel do
2   if surrogate creation cost  $< C_\S$  then
3      $S^s(\xi^r) = \text{createLocalSurrogates}(V_{h,s}, \text{semi-discrete PDE}, \text{tol})$ 
4   else
5      $S^s(\xi^r) = \text{createLocalSampler}(V_{h,s}, \text{semi-discrete PDE}, \text{matrix free} = \text{true})$ 
6 foreach sample  $\xi_k, k = 1, \dots, N$  in parallel do
7   obtain local samples  $(\xi_k^r)_{r=1}^M$  from  $\xi_k$ 
8   solve global interface problem(s) via parallel application of  $S^s(\xi_k^r)$  for  $s = 1, \dots, N_{\text{SD}}$ 
9   solve full decoupled local problems in parallel for  $s = 1, \dots, N_{\text{SD}}$ 
10  add solution sample contribution to approximate Q.o.I.( $u$ )

```

4.3 Parametric Schur complement method

As a first approach to non-overlapping domain decomposition methods, we consider the SCHUR complement method, see *e.g.* [46, Ch. 4-5] for details. For simplicity, the presentation is based on the elliptic linear equation (1) with the random dependence setting introduced in the beginning of this section. Given a physical discretization space $V_h \subset \mathcal{V} := H_{\Gamma_0}^1(D)$ spanned by a nodal LAGRANGE basis on a matching triangle (tetrahedral for $d = 3$) mesh of D , we consider a semi-discretization with respect to the physical coordinate x . Let us denote by Π the (primal) *interface*

$$\Pi = \cup_{s \neq s'} \partial D_s \cap \partial D_{s'},$$

consisting of faces ($d = 3$), edges and vertices with respect to the underlying mesh. Identifying the degrees of freedoms in V_h with topological entities, we can reorder those with regard to *local* contributions indexed by the letter L , corresponding to topological entities in the inner of D_s and on

Neumann parts $\overline{D_s} \cap \Gamma_1$ and to interacting primal interface contributions, indexed with the letter Π , for convenience. This semi-discretization of (1) leads to a structure of (35) with

$$\begin{aligned}\mathcal{A}(\xi(\omega)) &:= \begin{pmatrix} A_{LL} & A_{L\Pi} \\ A_{\Pi L} & A_{\Pi\Pi} \end{pmatrix} (\xi(\omega)), \\ u(\xi(\omega)) &:= \begin{pmatrix} u_L \\ u_\Pi \end{pmatrix} (\xi(\omega)), \quad F := \begin{pmatrix} f_L \\ f_\Pi \end{pmatrix}.\end{aligned}$$

Then, block GAUSSIAN elimination leads to an equivalent system to (35) given as

$$\tilde{\mathcal{A}}(\xi(\omega))u(\xi(\omega)) = \tilde{F}(\xi(\omega)), \quad (36)$$

where

$$\begin{aligned}\tilde{\mathcal{A}}(\xi(\omega)) &:= \begin{pmatrix} A_{LL} & A_{L\Pi} \\ 0 & S_{\Pi\Pi} \end{pmatrix} (\xi(\omega)), \\ \tilde{F}(\xi(\omega)) &:= \begin{pmatrix} f_L \\ \tilde{f}_\Pi(\xi(\omega)) \end{pmatrix}, \\ \tilde{f}_\Pi(\xi(\omega)) &:= f_\Pi - A_{\Pi L}(\xi(\omega))A_{LL}(\xi(\omega))^{-1}f_L.\end{aligned}$$

Let R_s be the rectangular restriction matrix which restricts the global degrees of freedom vector associated to Π to local degrees of freedom vectors associated to local interface entities on the mesh on D_s only. Since the mesh has no hanging nodes, the entries of each R_s are in $\{0, 1\}$. For each $s = 1, \dots, N_{\text{SD}}$, consider local assembled matrices $A_{LL}^s, A_{L\Pi}^s, A_{\Pi L}^s, A_{\Pi\Pi}^s$, associated to local physical discretization spaces on D_s . Note that for each active index (r, s) , these matrices have a parametric dependence on ξ^r . With the given ordering in (32) it follows that these matrices are given by

$$\begin{aligned}A_{LL}(\xi(\omega)) &= \text{blockdiag}(A_{LL}^1, \dots, A_{LL}^s, \dots, A_{LL}^{N_{\text{SD}}}), \\ A_{\Pi L}(\xi(\omega)) &= \text{blockdiag}(R_1, \dots, R_{N_{\text{SD}}}) [A_{\Pi L}^1, \dots, A_{\Pi L}^s, \dots, A_{\Pi L}^{N_{\text{SD}}}], \\ S_{\Pi\Pi}(\xi(\omega)) &= \sum_{s=1}^{N_{\text{SD}}} R_s S_{\Pi\Pi}^s R_s^T, \quad S_{\Pi\Pi}^s = A_{\Pi\Pi}^s - A_{\Pi L}^s A_{LL}^{s-1} A_{L\Pi}^s,\end{aligned}$$

where each matrix with index s only depends on $\xi^r(\omega)$ if $(r, s) \in \mathcal{I}_{\text{active}}$ and $A_{\Pi L} = A_{L\Pi}$ almost everywhere in Ω . In particular, for each active index (r, s) , we have

$$S_{\Pi\Pi}^s(\xi^r(\omega)) = A_{\Pi\Pi}^s(\xi^r(\omega)) - A_{\Pi L}^s(\xi^r(\omega))A_{LL}^s(\xi^r(\omega))^{-1}A_{L\Pi}^s(\xi^r(\omega)). \quad (37)$$

In the deterministic setting, (36) is solved by first iteratively solving for u_Π and second solving (in parallel) for interior contributions u_L^s with $u_L = [u_L^1, \dots, u_L^{N_{\text{SD}}}]$. The full matrix $S_{\Pi\Pi}$ is never formed explicitly. Its action on a vector involves the application of the smaller matrices $S_{\Pi\Pi}^s$. In the deterministic case, the latter might be realized by a LU decomposition of A_{LL}^s and we build local surrogate models $\hat{S}_{\Pi\Pi}^s \approx S_{\Pi\Pi}^s$. Depending on the regularity of the maps

$$\xi^r(\omega) \mapsto S_{\Pi\Pi}^s(\xi^r(\omega)) \quad (38)$$

and the input dimension of ξ^r , this might be realized by interpolation (e.g. sparse grid, lagrange interpolation) or (quasi)-best approximation techniques (tensor reconstruction, hPCE). We note that the construction of the surrogate models may be expensive if the number of local degrees of freedom

associated with $\Pi \cap D_s$ or the random dimension of ξ^r grows or if a lack of regularity is present. In a practical implementation, this cost factor has to be compared to the cost of a full sampling approach with several back and forward solves of the involved LU decompositions in the iterative process of the application of the SCHUR complement matrix. It is known that the condition number of a deterministic SCHUR complement matrix grows like $\infty/(\mathcal{H})$, where H is the diameter of the subdomains and h the maximal elementsize in the subdomains [46].

The proposed method is summarized in Algorithm 3.

Algorithm 3: Realization as parametric SCHUR complement method

input : \circ sample $\mathbf{y}_k := \xi_k(\omega) = [\xi_k^1, \dots, \xi_k^M](\omega)$,
 \circ local system surrogates for $\xi(\omega) \mapsto S_{\Pi\Pi}(\xi(\omega))$
 \circ local surrogates for preconditioner of (parametric) $S_{\Pi\Pi}$.
output: approximated realization of $u_k = u(\xi_k(\omega))$ or of subdomain parts $u_k^s = u_{k|D_s}$.

- 1 Compute right-hand side realization $\tilde{F}_k = [f_L, \tilde{f}_{\Pi,k}] = \tilde{F}(\xi_k(\omega))$ of (36) via system surrogates.
 - 2 Iteratively solve $S_{\Pi\Pi,k} u_{\Pi,k} = \tilde{f}_{\Pi,k}$ via PCG. The application of operator $S_{\Pi\Pi,k}$ and its preconditioner are based on evaluation of local surrogates.
 - 3 Solve block diagonal system $A_{LL,k} u_{L,k} = f_L - A_{L\Pi,k} u_{\Pi,k}$ in parallel.
-

4.4 Parametric FETI-DP

The *Finite Element Tearing and Interconnecting Dual-Primal* (FETI-DP) method is known to successfully balance the requirement of a minimal communication by a coarse space by keeping good convergence rates within the preconditioned conjugate gradient solution scheme. It was introduced in [19] and further developed in [46, 42, 41, 31, 30], see also the references therein for the purely deterministic case. The main idea is to translate the original problem into a dual problem in which the local iterates are not conforming (e.g. discontinuous in the H^1 framework), represented by most degrees of freedom associated with the domain interfaces and only a small number is strongly enforced to be conforming (e.g. continuous) opposite to the SCHUR complement method, where all (primal) d.o.f.s associated with the interface are globally constrained. This small number of constraints is associated with *primal* d.o.f.s while building the (global) coarse communication space. To enforce conformity of the method, the iteration solves for *Lagrange* multipliers λ , which construct the *dual variables*. In the case of convergence, this enforces conformity of the non-primal interface degrees of freedom. For further extensions of the coarse space design, e.g. including adaptivity, we refer to [29, 32].

For the sake of simplicity, we stay on the algebraic matrix level subject to the discretization of the symmetric model problem (1). For interpretation in a HILBERTIAN framework, we refer to [33] and for a formulation in intermediate approximation FE spaces to [46].

After choosing the set of interior, dual and primal degrees of freedom, marked by the subindices I , Δ and Π for a given physical discretization based on meshes on D_s that are aligned with each other on the subdomain interfaces, the structure of the system (35) is given by

$$\mathcal{A}(\xi(\omega)) := \begin{pmatrix} A_{LL} & A_{L\Pi} & \mathcal{J}_L^T \\ A_{\Pi L} & A_{\Pi\Pi} & \mathcal{J}_\Pi^T \\ \mathcal{J}_L & \mathcal{J}_\Pi & 0 \end{pmatrix} (\xi(\omega)),$$

$$u(\xi(\omega)) := \begin{pmatrix} u_L \\ u_\Pi \\ \lambda \end{pmatrix}, \quad b = \begin{pmatrix} f_L \\ f_\Pi \\ 0 \end{pmatrix}.$$

Here the subindex $L = [I, \Delta]$ merges the subindices I and Δ to *local* contributions. The jump

operators $\mathcal{J}_L = [\mathcal{J}_L^1, \dots, \mathcal{J}_L^{N_{SD}}]$, with $\mathcal{J}_L^s = [0, J_\Delta^s]$ and \mathcal{J}_Π , consisting of values in $\{-1, 0, 1\}$, are build such that the solution $[u_L, u_\Pi]$ vector yields a conforming approximation if $[\mathcal{J}_L, \mathcal{J}_\Pi][u_L, u_\Pi]^T = 0$. Introducing restriction operators R_Π^s similar to the SCHUR complement method, mapping local primal degrees of freedom to global d.o.f.s associated with index Π , sub-assembling with respect to the primal variables (thus eliminating the need of \mathcal{J}_Π) and application of GAUSSIAN block elimination leads to an equivalent formulation that reads

$$\tilde{\mathcal{A}}(\xi(\omega))\tilde{u}(\xi(\omega)) = \tilde{b}(\xi(\omega)), \quad (39)$$

where

$$\tilde{\mathcal{A}}(\xi(\omega)) := \begin{pmatrix} A_{LL} & \tilde{A}_{L\Pi} & \mathcal{J}_L^T \\ 0 & \tilde{S}_{\Pi\Pi} & -\tilde{S}_{\Pi\lambda} \\ 0 & 0 & F \end{pmatrix} (\xi(\omega)), \quad (40)$$

$$\tilde{u}(\xi(\omega)) := \begin{pmatrix} u_L \\ \tilde{u}_\Pi \\ \lambda \end{pmatrix}, \quad \tilde{b}(\xi(\omega)) := \begin{pmatrix} f_L \\ \tilde{b}_\Pi(\xi(\omega)) \\ \tilde{b}_\lambda(\xi(\omega)) \end{pmatrix}. \quad (41)$$

Here, it holds that $\tilde{u}_\Pi = \sum_{s=1}^{N_{SD}} R_\Pi^s u_\Pi^s$, with $u_\Pi = [u_\Pi^1, \dots, u_\Pi^{N_{SD}}]$, stemming from a rearrangement of global degrees of freedom. For $s = 1, \dots, N_{SD}$, similar to the SCHUR complement method, we introduce the locally assembled semi-discrete matrices $A_{LL}^s, A_{L\Pi}^s, A_{\Pi,L}^s, A_{\Pi\Pi}^s$ with dependence only on $\xi^r(\omega)$ if $(r, s) \in \mathcal{I}_{\text{active}}$. We then have the relation

$$\tilde{S}_{\Pi\Pi}(\xi(\omega)) := \tilde{A}_{\Pi\Pi} - \tilde{A}_{\Pi L} A_{LL}^{-1} \tilde{A}_{L\Pi} = \sum_{s=1}^{N_{SD}} R_\Pi^s \left(A_{\Pi\Pi}^s - A_{\Pi L}^s A_{LL}^{s-1} A_{L\Pi}^s \right) R_\Pi^{sT},$$

$$\tilde{S}_{\Pi\lambda}(\xi(\omega)) := \tilde{A}_{\Pi L} A_{LL}^{-1} \mathcal{J}_L^T = \sum_{s=1}^{N_{SD}} R_\Pi^s A_{\Pi L}^s A_{LL}^{s-1} \mathcal{J}_L^{sT},$$

with the random FETI-DP dual matrix F and right-hand side contributions such that

$$\begin{aligned} F(\xi(\omega)) &:= \mathcal{J}_L A_{LL}^{-1} \mathcal{J}_L^T + \tilde{S}_{\Pi\lambda}^T \tilde{S}_{\Pi\Pi}^{-1} \tilde{S}_{\Pi\lambda} \\ \tilde{b}_\Pi(\xi(\omega)) &:= \sum_{s=1}^{N_{SD}} R_\Pi^s (f_\Pi^s - A_{\Pi L}^s A_{LL}^{s-1} f_L^s), \\ \tilde{b}_\lambda(\xi(\omega)) &:= \mathcal{J}_L A_{LL}^{-1} f_L - \mathcal{J}_L A_{LL}^{-1} \tilde{A}_{L\Pi} \tilde{S}_{\Pi\Pi}^{-1} (\tilde{f}_\Pi - \tilde{A}_{\Pi L} A_{LL}^{-1} f_L) \\ &= \mathcal{J}_L A_{LL}^{-1} f_L - \tilde{S}_{\Pi\lambda}^T \tilde{S}_{\Pi\Pi}^{-1} \tilde{b}_\Pi. \end{aligned}$$

Note that for a better readability we omitted the parametric dependence of matrices on the right-hand sides of the above equations. Examining the occurring matrices, their dimensions and their random dependence on local random vectors $\xi^s(\omega)$, we now discuss the construction of surrogate models. In order to avoid multiple LU forward and backward substitutions within the iteration of the system $F\lambda = \tilde{b}_\lambda$, we aim for a lower total cost of computing and storing the surrogates for a given total number of samples. The parametric matrix F is build up from three contributions, which are discussed separately:

1 With the random dependence $A_{LL}^s = A_{LL}^s(\xi^r(\omega))$, $(r, s) \in \mathcal{I}_{\text{active}}$, recall that

$$\mathcal{J}_L A_{LL}^{-1} \mathcal{J}_L^T = \sum_{s=1}^{N_{SD}} \mathcal{J}_L^s A_{LL}^{s-1} \mathcal{J}_L^{sT}, \quad \mathcal{J}_L^s = [0, J_\Delta^s].$$

The inverse of A_{LL}^s can be seen as a 2×2 block matrix

$$A_{LL}^{s^{-1}} = \begin{pmatrix} B_{II}^s & B_{I\Delta}^s \\ B_{\Delta I}^s & B_{\Delta\Delta}^s \end{pmatrix}. \quad (42)$$

Due to the design of \mathcal{J}_L^s , only information of $B_{\Delta\Delta}$ contributes. Consequently, we aim for a surrogate of the mappings

$$\xi^r(\omega) \mapsto B_{\Delta\Delta}^s(\xi^r(\omega)), \quad \forall(r, s) \in \mathcal{I}_{\text{active}}. \quad (43)$$

The surrogates of this mappings involve the largest coefficient matrices, depending only on the local dual degrees of freedom.

- 2 We are now concerned with constructing surrogates to build $\tilde{S}_{\Pi\lambda}$. Note that with the notation in (42) we have

$$\begin{aligned} A_{\Pi L}^s A_{LL}^{s^{-1}} \mathcal{J}_L^{sT} &= (A_{\Pi I}^s \quad A_{\Pi \Delta}^s) \begin{pmatrix} B_{II}^s & B_{I\Delta}^s \\ B_{\Delta I}^s & B_{\Delta\Delta}^s \end{pmatrix} \begin{pmatrix} 0 \\ \mathcal{J}_\Delta^{sT} \end{pmatrix} \\ &= (A_{\Pi I}^s B_{I\Delta}^s + A_{\Pi \Delta}^s B_{\Delta\Delta}^s) \mathcal{J}_\Delta^{sT}. \end{aligned}$$

Thus, we aim for surrogates of the mapping

$$\xi^s(\omega) \mapsto [A_{\Pi I}^s B_{I\Delta}^s + A_{\Pi \Delta}^s B_{\Delta\Delta}^s](\xi^r(\omega)), \quad \forall(r, s) \in \mathcal{I}_{\text{active}}. \quad (44)$$

Coefficient matrices of the involved surrogates only depend on the number of local primal d.o.f.s times local dual d.o.f.s and are thus rather small if the coarse space is small.

- 3 The SCHUR complement matrix $\tilde{S}_{\Pi\Pi}$ is treated as in the parametric SCHUR complement method in Section 4.3 via surrogates of

$$\xi^r(\omega) \mapsto S_{\Pi\Pi}^s(\xi^r(\omega)), \quad \forall(r, s) \in \mathcal{I}_{\text{active}}, \quad (45)$$

whereas the coefficient matrix sizes only depend on local degrees of freedom associated to the coarse space and hence are rather small compared to the classic coarse space in the SCHUR complement method.

The right-hand side of the parametric system can also be computed via surrogates.

- 1 The local surrogates employed for the evaluation of $\tilde{b}(\xi(\omega))$ are given by

$$\xi^r \mapsto b_{II}^s(\xi^r(\omega)) := f_{II}^s - A_{\Pi L}^s(\xi^r(\omega)) A_{LL}^s(\xi^r(\omega))^{-1} f_L^s, \quad (46)$$

for all active indices (s, r) .

- 2 The computation of \tilde{b}_λ can be based on local surrogates

$$\xi^r(\omega) \mapsto B_{\Delta I}^s(\xi^r(\omega)) f_I^s + B_{\Delta\Delta}^s(\xi^r(\omega)) f_\Delta^s \quad (47)$$

for active indices (s, r) in addition to the surrogates for $\tilde{S}_{\Pi\lambda}$, $\tilde{S}_{\Pi\Pi}$ and \tilde{b} .

Note that all local surrogates can be computed in parallel and stored distributedly. The suggested approach is summarized in Algorithm 4.

Algorithm 4: Realization in parametric FETI-DP

input : ◦ sample $\mathbf{y}_k := \boldsymbol{\xi}_k(\omega) = [\boldsymbol{\xi}_k^1, \dots, \boldsymbol{\xi}_k^M](\omega)$,

◦ local based system surrogates for $\boldsymbol{\xi}(\omega) \mapsto [F, \tilde{S}_{\Pi\Pi}, \tilde{S}_{\Pi\lambda}](\boldsymbol{\xi}(\omega))$

◦ local based surrogates for preconditioner of (parametric) F .

output: approximated realization of $u_k = u(\boldsymbol{\xi}_k(\omega))$ or subdomain parts $u_k^s = u_k|_{D_s}$.

- 1 Compute rhs realisation $\tilde{b}_k = [f_L, \tilde{b}_{\Pi,k}, \tilde{b}_{\lambda,k}] = \tilde{b}(\boldsymbol{\xi}_k(\omega))$ (41) via surrogates (44)-(47).
 - 2 Iteratively solve $F_k \lambda_k = \tilde{b}_{\lambda,k}$ via a preconditioned CG method. The application of the operator F_k and its preconditioner are based on evaluating (43)-(45) and (53).
 - 3 Solve SCHUR complement system $\tilde{S}_{\Pi\Pi,k} \tilde{u}_{\Pi,k} = \tilde{b}_{\Pi,k} + \tilde{S}_{\Pi\lambda,k} \lambda_k$ via (45).
 - 4 Solve block diagonal system $A_{LL,k} u_{L,k} = f_L - \tilde{A}_{L\Pi,k} \tilde{u}_{\Pi,k} - \mathcal{J}_L^T \lambda_k$ in parallel.
-

The advantage of deterministic FETI-DP lies in its potential to lead to a *weakly scalable* algorithm that is enabled by a suitable choice of coarse space (associated with Π) and preconditioner P for the submatrix F [46]. In the context of domain decomposition techniques, the term *scalability* is associated with the iterative solution cost of the discrete system, which should not deteriorate when the number of subdomains grows. Let H denote the diameter of the subdomain and h the maximal diameter of the subdomain mesh cells. It can then be shown that

$$\kappa(P^{-1}F) \leq C \left(1 + \log \left(\frac{H}{h} \right) \right)^2, \quad (48)$$

where κ denotes the condition number, see *e.g.* [46] and the references therein. The construction of the scaled *lumped* and *DIRICHLET* preconditioner and its extension to the random case using surrogates is discussed in the next subsection 4.4.1.

4.4.1 Preconditioner

In what follows we introduce surrogates for two classic FETI-DP preconditioners, namely the *lumped* and the *Dirichlet* preconditioner P_{lumped}^{-1} and P_{Dir}^{-1} . These are given pointwise by

$$P_{\#}^{-1}(\boldsymbol{\xi}(\omega)) = \sum_{s=1}^{N_{\text{SD}}} W^s \mathcal{J}_{\Delta}^s M_{\#}^s \mathcal{J}_{\Delta}^{sT} W^s, \quad \# \in \{\text{lump}, \text{Dir}\}, \quad (49)$$

with $M_{\text{lump}} = A_{\Delta\Delta}^s$ and $M_{\text{Dir}} = A_{\Delta\Delta}^s - A_{\Delta I}^s A_{II}^{s-1} A_{I\Delta}^s$. Here, $M_{\#}^s = M_{\#}^s(\boldsymbol{\xi}^r(\omega))$ for all $(r, s) \in \mathcal{I}_{\text{active}}$. The diagonal scaling weight mappings W^s have a more involved parametric structure due to the coupling of neighboured random dependencies shown in (50).

We fix a subdomain D^s and let $D^{s'}$ be any neighboring subdomain such that there exist dual d.o.f.s Δ_i^s and $\Delta_j^{s'}$ in the local spaces associated with local meshes on those subdomains that both account for the same global dual degree of freedom. We collect those $D^{s'}$ into D_{Δ}^s , noting that $D^s \in D_{\Delta}^s$ per definition. Then, following [42], the diagonal scaling W^s is defined as

$$(W^s)_{ii} = \text{diag}(A_{\Delta\Delta}^s)_{ii} \left(\sum_{s': D^{s'} \in D_{\Delta}^s} \text{diag}(A_{\Delta\Delta}^{s'})_{jj} \right)^{-1}. \quad (50)$$

With this construction, the diagonal scaling enables the preconditioner to take material heterogeneities into account. An important observation is that if the assembled local dual matrices $A_{\Delta\Delta}^s$ and their

neighborhood counterparts $A_{\Delta\Delta}^{s'}$ depend on ξ^r and $\xi^{r'}$, respectively, then W^s is a matrix valued function depending on ξ^r and $\xi^{r'}$, so that a direct surrogate construction may be not applicable due to the sum of involved local parameter dimensions.

Since the underlying physical local meshes are fixed, we can work around this issue. For s' such that $D^{s'} \in D_{\Delta}^s$, we introduce diagonal matrices $W_{s'}^s$ with

$$(W_{s'}^s)_{ii} = \begin{cases} \text{diag}(A_{\Delta\Delta}^{s'})_{jj} & \exists j : \Delta_j^{s'}, \Delta_i^s \text{ share common global dual d.o.f} \\ 0, & \text{else.} \end{cases} \quad (51)$$

Then, we can compactly write

$$W^s = \text{diag}(A_{\Delta\Delta}^s) \left(\sum_{s': D^{s'} \in D_{\Delta}^s} W_{s'}^s \right)^{-1}, \quad (52)$$

where $W_{s'}^s = W_{s'}^s(\xi^{r'})$ for all $(r', s') \in \mathcal{I}_{\text{active}}$. With this construction, we may generate surrogate of the following maps, which depend only on local parameters,

$$\xi^r(\omega) \mapsto \begin{cases} M_{\#}^s(\xi^r(\omega)), & \# \in \{\text{lump}, \text{Dir}\} \\ \text{diag}(A_{\Delta\Delta}^s(\xi^r(\omega))), & \\ W_{s'}^s(\xi^r(\omega)), & D^{s'} \in D_{\Delta}^s, \end{cases} \quad \forall (r, s) \in \mathcal{I}_{\text{active}}, \quad (53)$$

and define the application of the preconditioner based on these local surrogates.

Remark 4.5. If the aim of the computation involves the recovering of approximate sample solutions over the whole domain, then A_{LL}^s needs to be inverted per sample separately, see Algorithm 4. In this situation, for each s , A_{LL}^s is assembled sample-wise such that $A_{\Delta\Delta}^s$ is accessible. Then, we propose to only build a surrogate for $\xi^r(\omega) \mapsto M_{\text{Dir}}^s(\xi^r(\omega))$ for $(r, s) \in \mathcal{I}_{\text{active}}$ as this map would introduce several inversions of A_{II}^{s-1} in the solution iteration scheme of a preconditioned conjugate gradient method.

Remark 4.6. In summary, we presented a pointwise surrogate approach, which for each sample up to surrogate precision enables weak-scalability based on the deterministic results. Alternatively, a fixed preconditioner such as the mean $\mathbb{E}[P_{\#}^{-1}]$ can be considered as in [10] for the SCHUR complement method.

4.4.2 Parametric FETI-DP for cluster sampling

In this subsection we consider cluster sampling (as a special case) that corresponds to a piecewise constant approximation of the involved parametric assembled discretization in the spirit of zero order gHPCE from subsection 3.2. While the discretization due to cost aspects is applicable to low local parametric dimensions only, it turns out that the resulting surrogates have a very simple structure. In this case, the surrogates are not needed to be build explicitly and the method involving its preconditioner is a simple generalization of the classic deterministic FETI-DP in all its algorithmic details, like the use of precomputed LU decompositions of the involved inverse matrix applications. We shall describe the benefits illustrated with the random FETI-DP matrix F .

Let (r, s) be active and consider the zero order gHPCE for any involved local random matrix M^s such that

$$M^s(\xi^r(\omega)) \approx M_0^s(\xi^r(\omega)) := \sum_{j \in \mathcal{J}} M_j^s \Psi_{0,j}(\xi^r(\omega)). \quad (54)$$

A key observation follows if M_j^s is invertible for all $j \in \mathcal{J}$. By the push-forward $\mu^r = \mathbb{P}_{\#\xi^r}$ and identification $\mathbf{y}^r = \xi^r(\omega)$ and $\Gamma^r = \cup_{j \in \mathcal{J}} \Gamma_j^r$, it holds pointwise

$$M^s(\mathbf{y}^r)^{-1} = (M_{j'}^s \Psi_{0,j'}(\mathbf{y}^r))^{-1}, \quad \mu^r\text{-a.e.}, \mathbf{y}^r \in \Gamma_{j'}^r. \quad (55)$$

As a consequence, e.g. the inverse of the SCHUR complement structure $S_{\Pi\Pi}^s(\xi^r(\omega))^{-1}$ has an easy form given as

$$S_{\Pi\Pi}^s(\xi^r(\omega)) = \sum_{j \in \mathcal{J}} S_{\Pi\Pi j}^s \Psi_{0,j}(\xi^r(\omega)), \quad (56)$$

where only one summand contributes to a realization of ξ^r . With that structure, one also gets for the s -th summand $R_{\Pi}^s A_{\Pi L}^s A_{LL}^{s-1} \mathcal{J}_L^{sT}$ in the definition of $\tilde{S}_{\Pi\lambda}$ that

$$[A_{\Pi L}^s A_{LL}^{s-1}](\mathbf{y}^r) = \left(\sum_{j \in \mathcal{J}} A_{\Pi L j}^s \Psi_{0,j}(\mathbf{y}^r) \right) \left(\sum_{j' \in \mathcal{J}} (A_{LL j'}^s \Psi_{0,j'}(\mathbf{y}^r))^{-1} \right) \quad (57)$$

$$= \sum_{j \in \mathcal{J}} A_{\Pi L j}^s (A_{LL j}^s)^{-1} \chi_{\Gamma_j^r}(\mathbf{y}^r), \quad (58)$$

with indicator function $\chi_{\Gamma_j^r}$. Thus, for a global realization, the application of F relies on precomputed factorizations of $A_{LL j}^s$ and storage of all involved coefficient matrices for $s = 1, \dots, N_{SD}$, and $j \in J$. This indicates a limiting factor if $|J|$ gets too large by the *curve of dimensionality*.

The piecewise constant approximation scheme in the stochastic space is suitable for domain-wise random fields $\omega \mapsto a(x, \omega) = a(x, X(\omega))$ parametrized by a discrete random variable X with finite dimensional image $\{x_1, \dots, x_{|J|}\}$. Such fields might be represented as

$$a(x, X(\omega)) = \varphi_0(x) + \sum_{j \in J} \pi_j(X(\omega)) \varphi_j(x), \quad (59)$$

with polynomials π_j with $\pi_j(x_i) = \delta_{ij}$ and functions φ_j in physical space. A special case of this is the *checkerboard material* with $\pi_0(y) = y$, $\pi_1(y) = 1 - y$, and $\varphi_j \equiv j$.

5 Numerical Experiments

We present some numerical validation of the proposed method for the partition of unity interpolation approach of Section 3.3. The implementation of the hybrid domain decomposition method for random domains was carried out as part of the open source ALEA library [13] with the deterministic FE backend FEniCS [20] for the assembly of local matrices. The approximation spaces for random coordinate space are realized with a custom implementation of hierarchical tree based decompositions of M -dimensional cells such as tensorized hyper quadrilaterals. Each such element then can be refined anisotropically by bisection separately in each coordinate direction. Additionally, a cell is refined into *macro-elements* (marked as gray in the figures below) and remaining hyper quadrilaterals if sub-areas are not necessary for further refinement in the marking process.

Two experiments based on the model problem (1) are considered with homogeneous DIRICHLET boundary conditions. In Section 5.1, we examine a smooth local parametric dependence with a challenge introduced by a non-linear coupling of random and physical coordinates. A random cookie problem as described in Example 2.9 representing non-smooth data is presented in Section 5.2.

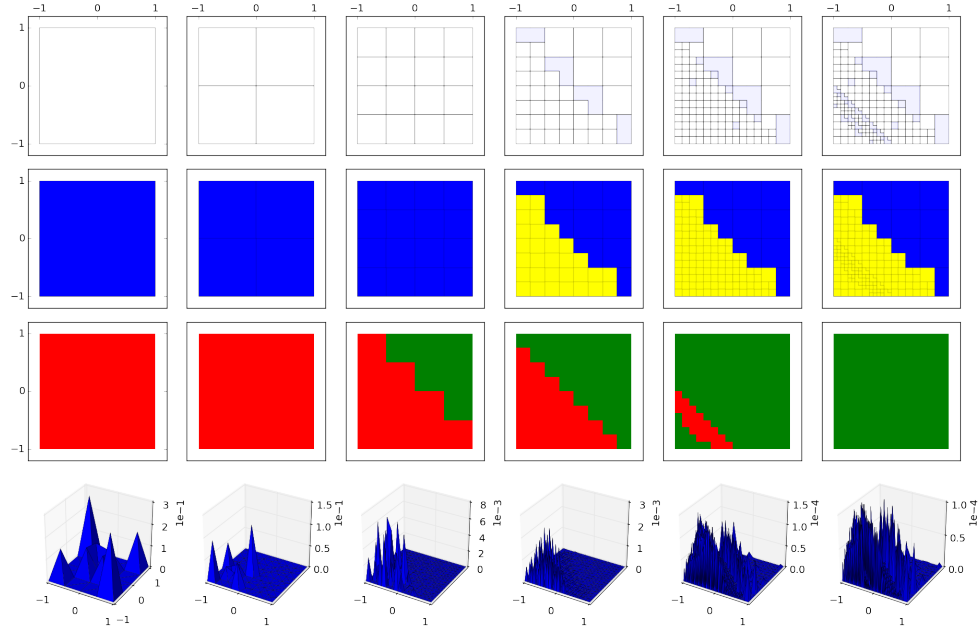


Figure 3: Adaptive surrogate construction based on macro-element anisotropic refinement procedure for $\xi^s \mapsto B_{DD}^s(\xi^s)$ for an inner square D_s with $\text{tol} = 10^{-4}$ and 100% trusted zone after 6 iterations.

The Figures 3-5 (respectively 9-11) serve to illustrate the adaptive surrogate generation. The figures from top to bottom show: the partitioned parametric domain I^s , employed polynomial degrees (4: blue, 3: yellow, 2 orange), trust/no-trust zones and local errors.

5.1 Smooth problem with non-linear coupling

We consider $D = [0, 1]^2$ and a partition of D into $N \times N$ subsquares D_s with $N = 3$, $x = (x_1, x_2)$. Our model for a smooth random field with a coupling of physical and stochastic coordinates is given as

$$a(x, \xi) = a(x, \xi^s(\omega)) = 1.1 + \sin(\alpha\pi(x_1\xi_1(\omega) + x_2\xi_2(\omega))), \quad x \in D_s, \quad (60)$$

with $\xi^s = (\xi_1^s, \xi_2^s)$, $\alpha = 0.7$ and independent $\xi_i^s \sim \mathcal{U}[-1, 1]$, for $i = 1, M = 2, s = 1, \dots, N_{\text{SD}} = 9$ resulting in a total of 18 random dimensions. In Figures 3-5, we illustrate the adaptive partitioning process of a local random image space $[-1, 1]^M$ based on Algorithm 1. In the experiment we utilize a physical discretisation with $p = 1$ FE on uniform 30×30 triangulations of D_s , $s = 1, \dots, N_{\text{SD}}$. The non-linear coupling of random and physical coordinates introduces a layer of the involved matrix valued random maps that differs for all $s = 1, \dots, 9$, also depending on the size of values taken in x . We illustrate the different structures in Figure 6 by final meshes obtained by the adaptive scheme. We point out that $\alpha = 2\pi$, or on larger domains D and thus related larger range of x , the surrogate construction becomes more involved and finer layers have to be resolved. In the numerical investigation, it is observed that given a $\text{tol} > 0$ for the local interface surrogates, the error between a sampled solution based on surrogates denoted by \hat{u}_h^k and its analogue (Monte Carlo) sample solution denoted by u_h^k is of higher order. The situation is illustrated in Figure 7 with a pointwise difference of order $\mathcal{O}(10^{-6})$ and $\|\hat{u}_h^k - u_h^k\|_{H_0^1(D)} / \|u_h^k\| \in \mathcal{O}(6 \times 10^{-5})$.

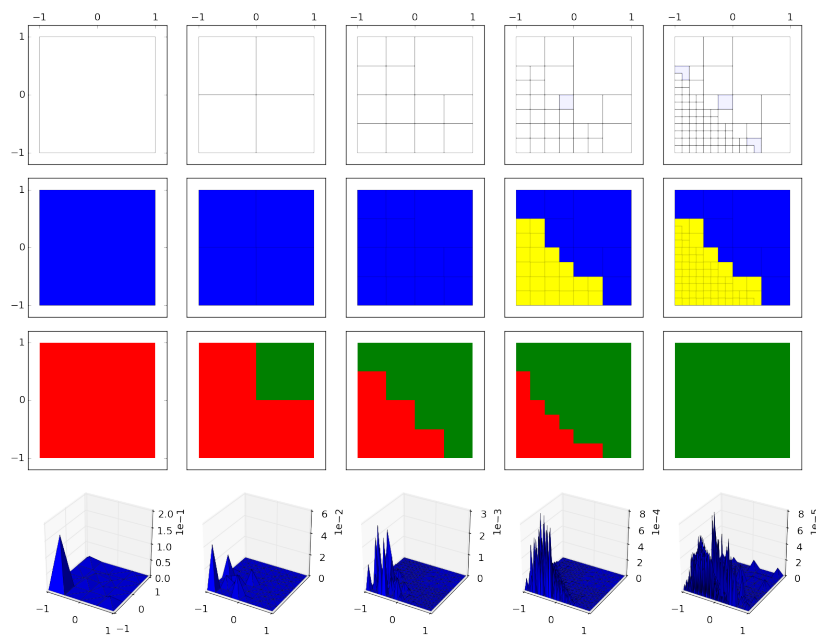


Figure 4: Adaptive surrogate construction procedure for $\xi^s \mapsto S_{II\lambda}^s(\xi^s)$ for an inner square D_s with $\text{tol} = 10^{-4}$ and 100% trusted zone after 5 iterations.

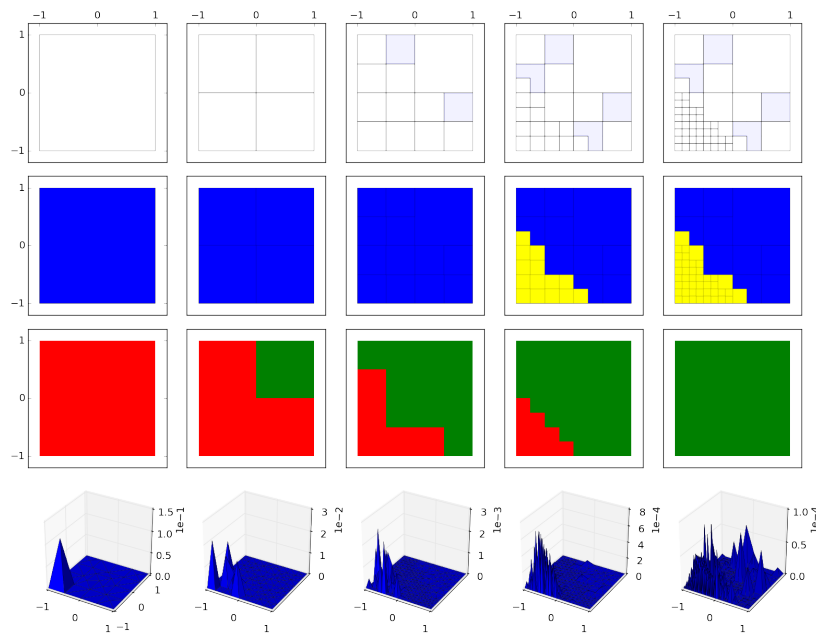


Figure 5: Adaptive surrogate construction procedure for $\xi^s \mapsto S_{PP}^s(\xi^s)$ for an inner square D_s with $\text{tol} = 10^{-4}$ and 100% trusted zone after 5 iterations.

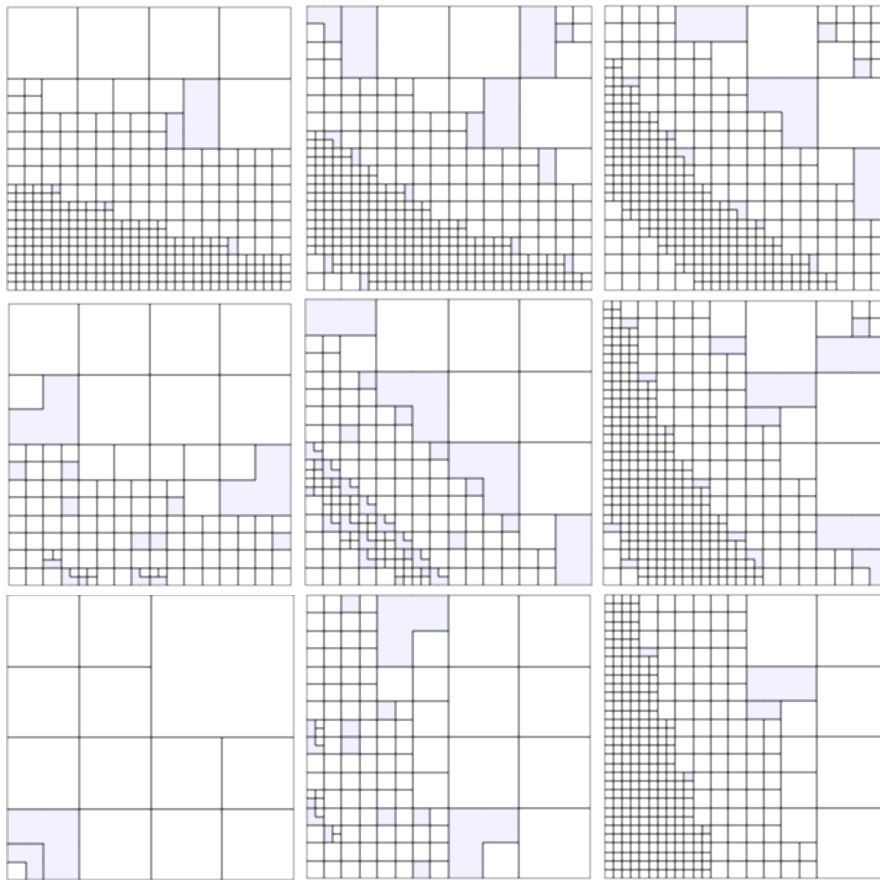


Figure 6: Final meshes on the surrogate random domain $\text{img } \xi^s = [-1, 1]^2$ for $s = 1, \dots, 9$ with $\text{tol} = 10^{-4}$ and resulting 100% trusted region for the maps $\xi^s \mapsto B_{DD}^s(\xi^s)$ using macro-elements (gray) and an anisotropic refinement. The polynomial degrees vary from 2 for very small to 4 for larger elements.

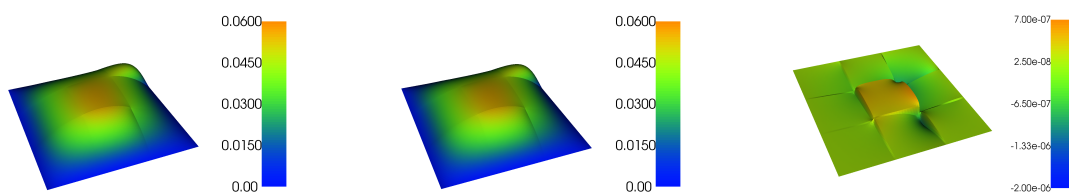


Figure 7: From left to right: MC sample, surrogate based sample and difference of globally reconstructed discrete solution for the problem in S 5.1 using a uniform 30×30 triangular mesh on each of the 3×3 subdomains.

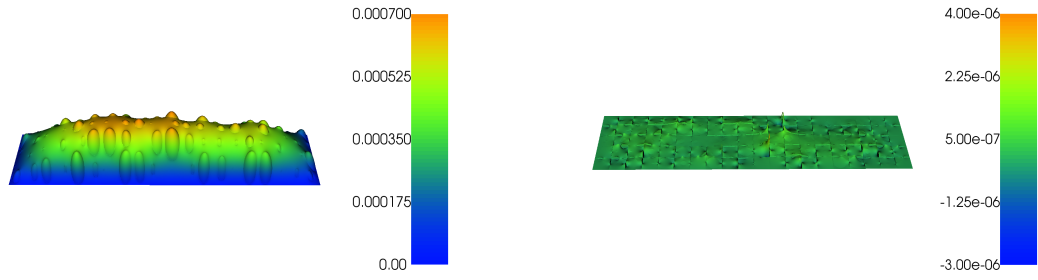


Figure 8: Left: Surrogate based sample \hat{u}_h^k for the random cookie problem on 20×5 subdomains using $p = 1$ FE on local uniform 40×40 triangular meshes on D_s . Right: Pointwise difference to MC sampled discrete solution u_h^k . Local surrogates build with $\text{tol} = 10^{-2}$ leading to relative $H_0^1(D)$ errors of $\|\hat{u}_h^k - u_h^k\|_{H_0^1(D)} / \|u_h^k\| \in \mathcal{O}(9 \times 10^{-3})$.

5.2 Cookie problem, model problem for more general composite materials

We consider a rectangular domain $D = [0, W] \times [0, H]$ with parameters $H, W > 0$ such that D can be decomposed into squares D_s for $s = 1, \dots, N_{\text{SD}} = N_H N_W$, where N_H (respectively N_W) denotes the number of squares in their respective direction.

Remark 5.1. For the physical discretization a fixed uniform (local) triangular mesh is used implicitly for each realization of the composite structure. In particular, given a realization of the composite, the mesh does not resolve the jump in the coefficient, which in a deterministic setting is critical from an accuracy point of view. Note that, to benefit from using such a fixed mesh, the FE basis functions can be enriched by an element-wise basis function with a jump in the gradient of the discrete basis function as described in [27]. With this, the presented technique exhibits a better approximation quality with respect to the solution u . On each square domain D_s , the random field \mathbb{P} -a.e. is described as

$$a(x, \omega) = a(x, \xi^s(\omega)) = \chi_{B(\xi^s(\omega))}(x) + 20(1 - \chi_{B(\xi^s(\omega))}(x)), \quad x \in D_s. \quad (61)$$

Here, $B^s(\xi^s(\omega))$ denotes a random ball modelled by a random radius r and a random x position such that $[r, x] = \varphi^s(\xi_1^s(\omega), \xi_2^s(\omega))$ with a map φ^s chosen such that $B(\xi^s(\omega))$ is uniformly bounded away from ∂D_s by a given distance as in Example 2.9. By a push-forward we may identify $\mathbf{y}^s = \xi^s(\omega)$ and interpret $\mathbf{y}^s \mapsto a(\cdot, \mathbf{y}^s)$ as an element in $L^2([-1, 1]^2; L^\infty(D))$. We stress that $a \notin \mathcal{C}([-1, 1]^2; L^\infty(D))$ but $a \in L^\infty([-1, 1]^2; L^\infty(D))$. The defined composite material coefficient lacks regularity in the random as well as the physical coordinates. Note that the full random dimension is $M' = 2N_H N_W$, e.g. with $M = 200$ for 20×5 squares as illustrated in Figure 8. Due to the same structure of the domain-wise non-periodic material description for the homogeneous DIRICHLET problem, it suffices to compute local surrogates for 9 subdomains only (4 associated to each corner and edge, 1 inner domain). The adaptive procedure is illustrated for the inner domain case in Figures 9-11. We point out the remarkable refinement pattern towards the right domain side. The right interface corresponds to the case of maximal radius of the random ball, the top and bottom interface correspond to the maximal displacement of the ball. Due to the surrogate construction based on a semi-discretization, given sufficiently fine physical meshes, the intersection of the random ball and the support of the basis functions associated locally to the boundary shrinks. Thus, the dependence of the non-smooth influence gets smaller. Furthermore, we observe a constant error for $B_D D$ in Figure 9 that accounts for the remaining support interaction and exhibits a notable very slow decrease. This interaction is further illustrated in Figure 12, when solving for a smaller tolerance $\text{tol} = 10^{-3}$.

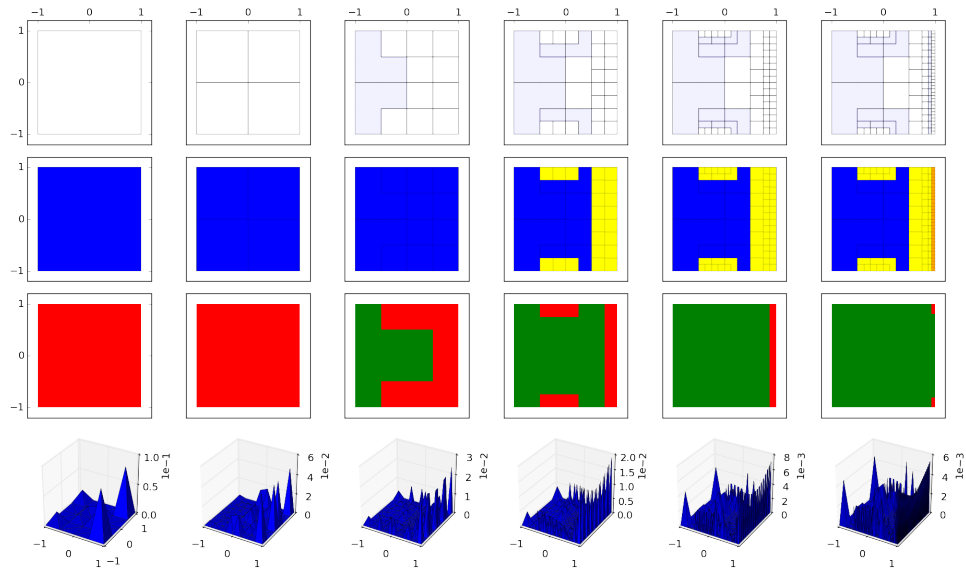


Figure 9: Adaptive surrogate construction based on macro-element anisotropic refinement procedure for $\xi^s \mapsto B_{DD}^s(\xi^s)$ for a inner square D_s with $\text{tol} = 0.5 \times 10^{-2}$. 99.41% trusted zone after 6 iterations.

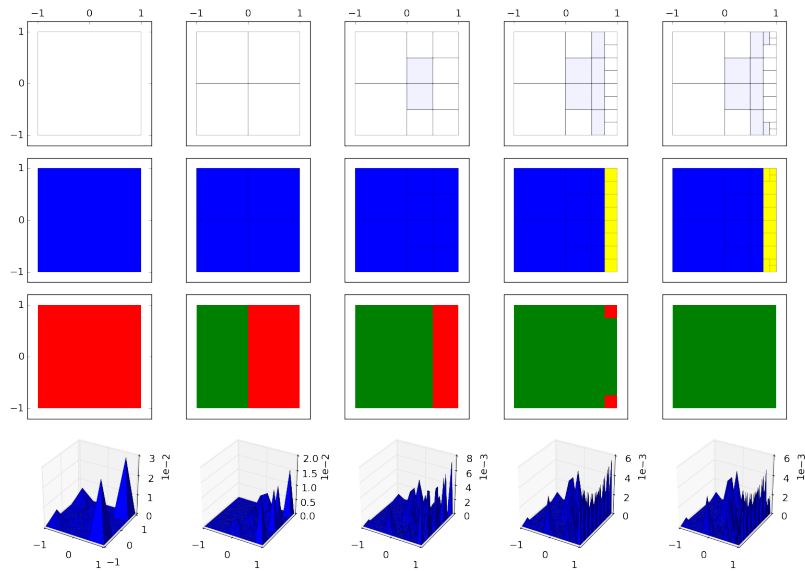


Figure 10: Adaptive surrogate construction procedure for $\xi^s \mapsto S_{II\lambda}^s(\xi^s)$ for a inner square D_s with $\text{tol} = 0.5 \times 10^{-2}$. 100% trusted zone after 5 iterations.

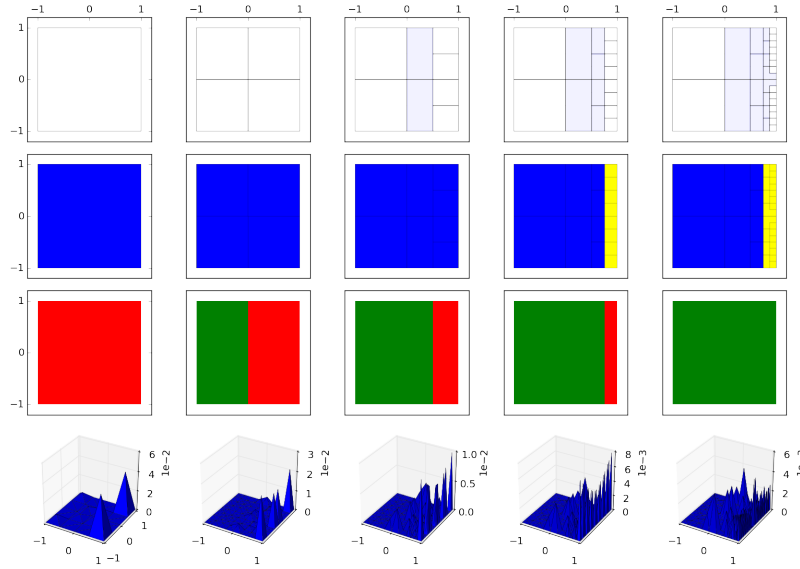


Figure 11: Adaptive surrogate construction procedure for $\xi^s \mapsto S_{PP}^s(\xi^s)$ for a inner square D_s with $\text{tol} = 0.5 \times 10^{-2}$. 100% trusted zone after 5 iterations.

Remark 5.2. In the numerical experiments, building the surrogate $\xi^s \mapsto A_{LL}^s(\xi^s)^{-1}$ leads to massive uniform refinements with an (arbitrarily) slow error decrease. However, the involved interface operators are observed to exhibit rather smooth sub-areas in the parametric space with remaining small non-trusted areas.

Acknowledgements

The authors would like to thank Prof. Hermann Matthies for pointing out Remark 2.10.

References

- [1] C. Amrouche, C. Conca, A. Ghosh, and T. Ghosh. Uniform $W^{1,p}$ estimate for elliptic operator with robin boundary condition in \mathcal{C}^1 domain. *arXiv preprint arXiv:1805.09519*, 2018.
- [2] I. Babuška and P. Chatzipantelidis. On solving elliptic stochastic partial differential equations. *Comput. Methods Appl. Mech. Engrg.*, 191(37-38):4093–4122, 2002.
- [3] I. Babuška, R. Tempone, and G. E. Zouraris. Solving elliptic boundary value problems with uncertain coefficients by the finite element method: the stochastic formulation. *Comput. Methods Appl. Mech. Engrg.*, 194(12-16):1251–1294, 2005.
- [4] M. Bachmayr, A. Cohen, and W. Dahmen. Parametric pdes: sparse or low-rank approximations? *IMA Journal of Numerical Analysis*, 38(4):1661–1708, 2017.

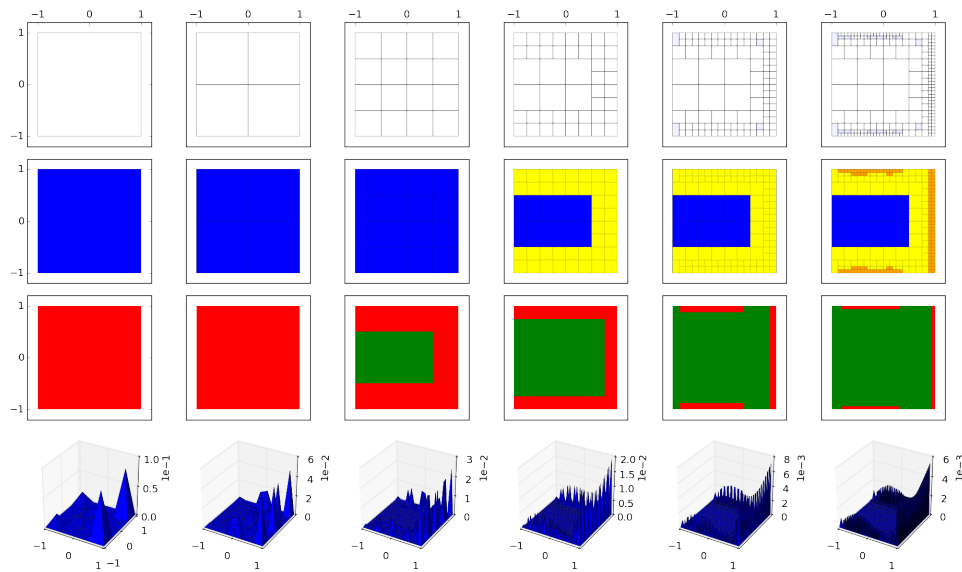


Figure 12: Adaptive procedure for B_{DD}^s associated to an inner domain D_s with $\text{tol} = 10^{-3}$. The maximal displacement areas and the maximal radius areas dominate the error and remain non-trusted. After 6 iterations a trusted area of 93.35% is obtained.

- [5] M. Bachmayr, R. Schneider, and A. Uschmajew. Tensor networks and hierarchical tensors for the solution of high-dimensional partial differential equations. *Foundations of Computational Mathematics*, 16(6):1423–1472, 2016.
- [6] A. Barth and A. Stein. A study of elliptic partial differential equations with jump diffusion coefficients. *arXiv preprint arXiv:1712.04876*, 2017.
- [7] A. Bonito, R. A. DeVore, and R. H. Nochetto. Adaptive finite element methods for elliptic problems with discontinuous coefficients. *SIAM Journal on Numerical Analysis*, 51(6):3106–3134, 2013.
- [8] M. Chevreuil, A. Nouy, and E. Safatly. A multiscale method with patch for the solution of stochastic partial differential equations with localized uncertainties. *Computer Methods in Applied Mechanics and Engineering*, 255:255–274, 2013.
- [9] A. A. Contreras, P. Mycek, O. Le Maître, F. Rizzi, B. Debusschere, and O. M. Knio. Parallel domain decomposition strategies for stochastic elliptic equations—part a: Local kl representations, 2016.
- [10] A. A. Contreras, P. Mycek, O. P. Le Maître, F. Rizzi, B. Debusschere, and O. M. Knio. Parallel domain decomposition strategies for stochastic elliptic equations part b: Accelerated monte carlo sampling with local pc expansions. *SIAM Journal on Scientific Computing*, 40(4):C547–C580, 2018.
- [11] C. F. Dunkl and Y. Xu. *Orthogonal polynomials of several variables*. Number 155. Cambridge University Press, 2014.
- [12] M. Eigel, C. J. Gittelsohn, C. Schwab, and E. Zander. Adaptive stochastic Galerkin FEM. *Comput. Methods Appl. Mech. Engrg.*, 270:247–269, 2014.

- [13] M. Eigel, R. Gruhlke, M. Marschall, P. Trunschke, and E. Zander. Alea - a python framework for spectral methods and low-rank approximations in uncertainty quantification.
- [14] M. Eigel, M. Marschall, M. Pfeffer, and R. Schneider. Adaptive stochastic galerkin fem for lognormal coefficients in hierarchical tensor representations. *arXiv preprint arXiv:1811.00319*, 2018.
- [15] M. Eigel and C. Merdon. Local equilibration error estimators for guaranteed error control in adaptive stochastic higher-order galerkin finite element methods. *SIAM/ASA Journal on Uncertainty Quantification*, 4(1):1372–1397, 2016.
- [16] M. Eigel, M. Pfeffer, and R. Schneider. Adaptive stochastic Galerkin FEM with hierarchical tensor representations. *Numerische Mathematik*, 136(3):765–803, Jul 2017.
- [17] M. Eigel, R. Schneider, P. Trunschke, and S. Wolf. Variational monte carlo-bridging concepts of machine learning and high dimensional partial differential equations. *arXiv preprint arXiv:1810.01348*, 2018.
- [18] O. G. Ernst, A. Mugler, H.-J. Starkloff, and E. Ullmann. On the convergence of generalized polynomial chaos expansions. *ESAIM: Mathematical Modelling and Numerical Analysis*, 46(2):317–339, 2012.
- [19] C. Farhat, M. Lesoinne, P. LeTallec, K. Pierson, and D. Rixen. Feti-dp: a dual-primal unified feti method—part i: A faster alternative to the two-level feti method. *International journal for numerical methods in engineering*, 50(7):1523–1544, 2001.
- [20] FEniCS Project - Automated solution of Differential Equations by the Finite Element Method.
- [21] L. Grasedyck, D. Kressner, and C. Tobler. A literature survey of low-rank tensor approximation techniques. *GAMM-Mitteilungen*, 36(1):53–78, 2013.
- [22] M. Griebel. Adaptive sparse grid multilevel methods for elliptic pdes based on finite differences. *Computing*, 61(2):151–179, 1998.
- [23] K. Gröger. A $W^{1,p}$ -estimate for solutions to mixed boundary value problems for second order elliptic differential equations. *Mathematische Annalen*, 283(4):679–687, 1989.
- [24] R. Gruhlke, M. Eigel, D. Hömberg, M. Drieschner, and Y. Petryna. A hybrid stochastic domain decomposition method for partial differential equations with localised possibly rough random data. *PAMM*, 18(1):e201800434, 2018.
- [25] W. Hackbusch. *Tensor spaces and numerical tensor calculus*, volume 42. Springer Science & Business Media, 2012.
- [26] M. Hadigol, A. Doostan, H. G. Matthies, and R. Niekamp. Partitioned treatment of uncertainty in coupled domain problems: A separated representation approach. *Computer Methods in Applied Mechanics and Engineering*, 274:103–124, 2014.
- [27] A. Ibrahimbegovic. *Nonlinear solid mechanics: theoretical formulations and finite element solution methods*, volume 160. Springer Science & Business Media, 2009.
- [28] D. J.-C. Kenig. The inhomogeneous dirichlet problem in lipschitz domains. *J. funct. Anal*, 130(1):161–219, 1995.

- [29] A. Klawonn, P. Radtke, and O. Rheinbach. Feti-dp methods with an adaptive coarse space. *SIAM Journal on Numerical Analysis*, 53(1):297–320, 2015.
- [30] A. Klawonn, O. Rheinbach, and O. B. Widlund. An analysis of a feti-dp algorithm on irregular subdomains in the plane. *SIAM Journal on Numerical Analysis*, 46(5):2484–2504, 2008.
- [31] A. Klawonn and O. B. Widlund. Dual-primal feti methods for linear elasticity. *Communications on Pure and Applied Mathematics: A Journal Issued by the Courant Institute of Mathematical Sciences*, 59(11):1523–1572, 2006.
- [32] M. J. Kühn. *Adaptive FETI-DP and BDDC methods for highly heterogeneous elliptic finite element problems in three dimensions*. PhD thesis, Universität zu Köln, 2018.
- [33] J. Mandel and B. Sousedík. Bddc and feti-dp under minimalist assumptions. *Computing*, 81(4):269–280, 2007.
- [34] Y. Marzouk, T. Moselhy, M. Parno, and A. Spantini. An introduction to sampling via measure transport. *arXiv preprint arXiv:1602.05023*, 2016.
- [35] N. G. Meyers. An l^p -estimate for the gradient of solutions of second order elliptic divergence equations. *Annali della Scuola Normale Superiore di Pisa-Classe di Scienze*, 17(3):189–206, 1963.
- [36] L. Mu and G. Zhang. A Domain-Decomposition Model Reduction Method for Linear Convection-Diffusion Equations with Random Coefficients. *arXiv e-prints*, page arXiv:1802.04187, Feb. 2018.
- [37] F. Nobile, R. Tempone, and C. G. Webster. A sparse grid stochastic collocation method for partial differential equations with random input data. *SIAM Journal on Numerical Analysis*, 46(5):2309–2345, 2008.
- [38] A. Nouy. Low-rank tensor methods for model order reduction. *Handbook of uncertainty quantification*, pages 857–882, 2017.
- [39] S. Oladyshkin and W. Nowak. Data-driven uncertainty quantification using the arbitrary polynomial chaos expansion. *Reliability Engineering & System Safety*, 106:179–190, 2012.
- [40] S. Rahman. Wiener–hermite polynomial expansion for multivariate gaussian probability measures. *Journal of Mathematical Analysis and Applications*, 454(1):303–334, 2017.
- [41] O. Rheinbach. Parallel scalable iterative substructuring: Robust exact and inexact feti-dp methods with applications to elasticity [phd thesis]. *Essen (Germany): University of Duisburg-Essen, Essen*, 2006.
- [42] D. J. Rixen and C. Farhat. A simple and efficient extension of a class of substructure based preconditioners to heterogeneous structural mechanics problems. *International Journal for Numerical Methods in Engineering*, 44(4):489–516, 1999.
- [43] C. Schwab. *P-and Hp-Finite Element Methods: Theory and Applications in Solid and Fluid Mechanics (Numerical Mathematics and Scientific Computation)*. Oxford University Press, New York, 1999.
- [44] W. Subber and A. Sarkar. Dual-primal domain decomposition method for uncertainty quantification. *Computer Methods in Applied Mechanics and Engineering*, 266:112–124, 2013.

- [45] L. Tartar. *An introduction to Sobolev spaces and interpolation spaces*, volume 3. Springer Science & Business Media, 2007.
- [46] A. Toselli and O. Widlund. *Domain decomposition methods-algorithms and theory*, volume 34. Springer Science & Business Media, 2006.
- [47] H. Triebel. Theory of function spaces ii. *Bull. Amer. Math. Soc*, 31:119–125, 1994.
- [48] X. Wan and G. E. Karniadakis. An adaptive multi-element generalized polynomial chaos method for stochastic differential equations. *Journal of Computational Physics*, 209(2):617–642, 2005.
- [49] D. Xiu and G. E. Karniadakis. The wiener–askey polynomial chaos for stochastic differential equations. *SIAM journal on scientific computing*, 24(2):619–644, 2002.